



Escola d'Enginyeria de Telecomunicació i
Aeroespacial de Castelldefels

UNIVERSITAT POLITÈCNICA DE CATALUNYA

MASTER THESIS

TITLE: LTE Performance Evaluation with Realistic Channel Quality Indicator Feedback

MASTER DEGREE: Master in Science in Telecommunication Engineering & Management

AUTHOR: Mathew William Churchman Barata

DIRECTOR: Mario García Lozano

DATE: April 29th 2011

TÍTULO: LTE Performance Evaluation with Realistic Channel Quality Indicator Feedback

TITULACIÓN: Master in Science in Telecommunication Engineering & Management

AUTOR: Mathew William Churchman Barata

DIRECTOR: Mario García Lozano

FECHA: 29 de abril de 2011

Resumen

En el contexto de las comunicaciones móviles, la disponibilidad de nuevos servicios y aplicaciones móviles conjuntamente con la constante evolución de los terminales móviles concluyen en la necesidad de una mayor velocidad de transmisión. Para poder cumplir con estas expectativas, los operadores de telefonía móvil están continuamente optimizando y actualizando sus redes. La evolución de UMTS (Universal Mobile Telecommunications System), LTE (Long Term Evolution) parece ser el camino a seguir a corto plazo.

El objetivo de este proyecto es estudiar el comportamiento de la asignación de recursos radio en LTE bajo condiciones realistas. La asignación o *scheduling* de recursos es un proceso clave para aprovechar correctamente los recursos radio. Se pueden identificar dos tipos de asignaciones, la oportunista, donde se considera el estado del canal radio para hacer la mejor asignación posible, y el no oportunista, donde no se tiene en cuenta esta información.

Como la opción oportunista se adapta a las condiciones del canal radio, requiere la transmisión de un cierto nivel de señalización por parte de los usuarios para informar de cómo evoluciona el canal con el tiempo. Uno de los objetivos de este proyecto es evaluar el comportamiento del sistema bajo diferentes niveles de retroalimentación. Para hacer esto se han programado y simulado diferentes métodos de reportes del canal (CQI reporting methods). Para conseguir este objetivo es obvio que se necesita del segundo: programar y simular de la manera más realista posible el canal radio de LTE.

La metodología seguida ha sido fundamentalmente la programación de diferentes modelos matemáticos y algoritmos y su simulación. Concretamente, una de las tareas principales ha sido extender una plataforma software del grupo de investigación Wicomtec para permitir resultados más realistas mediante simulaciones dinámicas sobre un canal dinámico.

TITLE: LTE Performance Evaluation with Realistic Channel Quality Indicator Feedback

MASTER DEGREE: Master in Science in Telecommunication Engineering & Management

AUTHOR: Mathew William Churchman Barata

DIRECTOR: Mario García Lozano

DATE: April 29th 2011

Overview

In the context of mobile communications, the availability of new services and mobile applications along with the constant evolution in terminals run up the need of higher data rates. In order to fulfill such expectations, mobile operators are continually optimizing and upgrading their networks. The Long Term Evolution (LTE) of the Universal Mobile Telecommunications System (UMTS) seems to be the path to follow in a very short term.

The objective of this project is to study the behaviour of the radio resource assignment in LTE under realistic conditions. The scheduling is a key process in the functioning of the radio interface. Thus, two types of schedulers can be identified, the opportunistic, where the scheduler considers the state of the radio channel to make the best allocation possible, and the non-opportunistic, where the allocation has no knowledge of the radio channel's state.

As the opportunistic option adapts to the radio channel conditions it requires the transmission of a certain level of signalling from users informing about how the channel evolves along time. One of the objectives of this project is to evaluate the system performance under different degrees of feedback. To do this, different CQI reporting methods have been programmed and simulated. So, to achieve this objective it is obvious that a second one is necessary: program and simulate in a more realistic way the LTE radio channel.

The followed methodology has been fundamentally the programming of different mathematical models and algorithms, as well as its simulation. In concrete, one of the main tasks in this work has been to extend a software platform of the research group Wicomtec to obtain more realistic results through dynamic simulations over a dynamic radio channel.

INDEX

CHAPTER 1. INTRODUCTION AND PROBLEM STATEMENT	1
1.1 Introduction	1
1.1.1 LTE Throughput Rates	2
1.1.2 OFDMA and Scheduling.....	3
1.2 Problem statement	4
CHAPTER 2. CHANNEL IMPLEMENTATION	7
2.1 Radio channel phenomena	7
2.1.1 Small-scale fading: Slow fading vs. fast fading	8
2.1.2 Small-scale fading: Frequency-selective fading vs. flat fading.....	9
2.1.3 LTE case: Frequency-selective but flat per subcarrier.....	10
2.2 Necessity of channel simulation in a LTE system simulator	11
2.2.1 Opportunistic scheduling in LTE.....	11
2.2.2 Channel state information for scheduling and link adaptation	13
2.3 Channel simulation strategies.....	15
2.3.1 Sum-of-Sinusoids Simulators	15
2.3.2 Filtered Gaussian Noise Simulators.....	16
2.3.2.1 Time filtering. Jakes Doppler Spectrum	16
2.3.2.1.1 Generation of the filter in time	18
2.3.2.1.2 Generation of the filter in frequency	19
2.3.2.2 Frequency filtering. Young's and Bealieu's IDFT Model	20
2.3.2.3 Auto-regressive filter.....	22
2.3.3 Chosen and implemented filter.....	23
CHAPTER 3. SIMULATOR.....	25
3.1 C++ Channel Simulator application introduction	25
3.2 Channel simulator	26
3.2.1 Reduction of the channel's values.....	27
3.2.1.1 95% values of the CDF.....	28
3.2.1.2 Alternative to the CDF procedure.....	28
3.2.2 Quantification.....	29
3.2.3 Final Results.....	30
3.2.4 Channel smooth	31
CHAPTER 4. DEVELOPMENT OF A DYNAMIC LTE SIMULATION PLATFORM	33
4.1 System simulator	33
4.1.1 User's movement and layout reduction	33
4.1.2 Reference signals.....	35
4.1.2.1 Reference signals in LTE	35
4.1.2.1.1 UE-specific RSs.....	36
4.1.2.1.2 Implemented RSs	36
4.1.3 CQI Feedback compression schemes	38
4.1.3.1 Aperiodic CQI Reporting.....	38
4.1.3.2 Periodic CQI Reporting.....	40
4.1.4 Hybrid ARQ	41
4.1.4.1 HARQ implementation.....	41

CHAPTER 5. SIMULATIONS	45
5.1 Fast fading channel parameters	45
5.2 Simulation parameters	46
5.3 Performance evaluation	46
5.3.1 Ideal CQI feedback.....	47
5.3.2 Wideband CQI feedback	48
5.3.3 UE-selected sub-band feedback	49
CONCLUSIONS.....	53
ACRONYMS	55
REFERENCES.....	59
ANNEX A	i
A.1 Evolution of mobile communications	i
A.1.1 First generation.....	i
A.1.2 Second generation	ii
A.1.3 Third generation	iii
A.1.4 Fourth generation	v
A.1.4.1 Basic System Architecture Configuration	v
A.2 Simulation results	vii
A.2.1 Ideal static LTE system simulator results	vii
A.2.2 Assigned transport format (CQI)	vii
A.3 Simulation parameters	ix
A.3.1 Layout and users	ix
A.3.2 Simulation	x
A.3.3 OFDMA.....	x
A.3.4 Classes.....	xi
A.3.5 RRM.....	xi
A.3.6 Sites/Sectors	xii
A.3.7 Wireless Channel	xii
A.3.8 PHY-MAC	xiii
A.3.9 CSI.....	xiii
A.4 LTE frequency bands	xiv

CHAPTER 1. INTRODUCTION AND PROBLEM STATEMENT

In a world where the virtual contents increase day by day, the desire to access to these contents from everywhere also increases and it is a key factor that users look for in a telecommunications operator. As fixed communications prevent mobility, the evolution of mobile communications aims to provide faster access to data and multimedia services. This is achieved by developing new standards.

1.1 Introduction

Mobile communications, as fixed communications, originated from voice telephony. The number of subscribers increased, so the technologies and standards evolved to provide this service to a larger amount of users, improving the quality as well as the resource management, evolving from analogue to digital and modifying the users multiplexing in order to obtain a better efficiency given the radio resources.

With time, this service has less importance, as data and multimedia services increased in demand and also in the number of broadband subscribers. This happened first in fixed and then in mobile communications, leading to a point where mobility between networks is also necessary. Therefore, 4th generation is expected to provide broadband, large capacity, high speed data transmission, providing users with high quality video, 3D graphic animation games and audio services. See Figure 1.1.

Since this project is framed in the context of the Long Term Evolution (LTE) of current UMTS (Universal Mobile Telephone System) systems, a short overview of this system is given just before posing the objectives of the project. Section A.1 from Annex A gives a complete overview of the evolution of mobile communications, from the first analogue cellular one to the fourth generation which implements LTE.

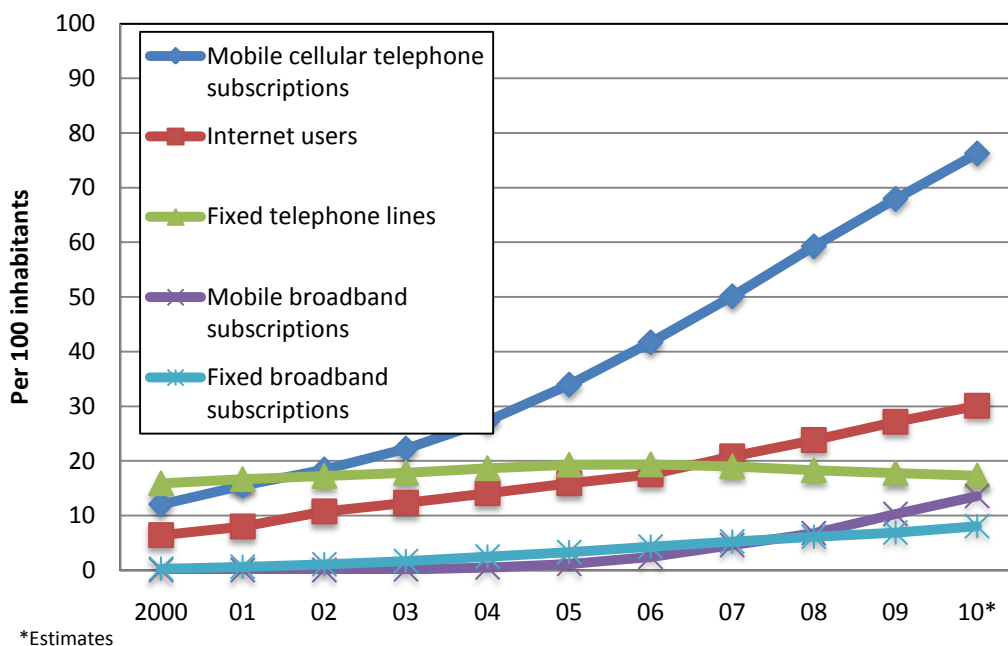


Figure 1.1: Global ICT developments, 2000-2010.*Source: ITU World Telecommunication /ICT Indicators database

3GPP has completed the specification for LTE as part of Release 8. LTE will allow operators to achieve even higher peak throughputs in higher spectrum BW.

LTE uses Orthogonal Frequency Division Multiple Access (OFDMA) on the DL, which is well suited to achieve high peak data rates in high-spectrum bandwidth (BW). WCDMA radio technology is basically as efficient as Orthogonal Frequency Division Multiplexing (OFDM) for delivering peak data rates of about 10 Mbps in 5 MHz of BW. Achieving peak rates in the 100 Mbps range with wider radio channels, however, would result in highly complex terminals, and it is not practical with current technology. This is where OFDM provides a practical implementation advantage. Scheduling approaches in the frequency domain can also minimize interference, thereby boosting spectral efficiency. The OFDMA approach is also highly flexible in channelization, and LTE will operate in various radio channel sizes ranging from 1.4 to 20 MHz.

On the uplink, however, a pure OFDMA approach results in high Peak to Average Ratio (PAR) of the signal, which compromises power efficiency and, ultimately, battery life. Hence, LTE uses an approach called Single-carrier FDMA (SC-FDMA), which is somewhat similar to OFDMA, but has a 2 to 6 dB PAR advantage over the OFDMA method used by other technologies such as WiMAX (Worldwide Interoperability for Microwave Access).

LTE capabilities include:

- DL peak data rates up to 326 Mbps with 20 MHz BW.
- Uplink peak data rates up to 86.4 Mbps with 20 MHz BW.
- Operation in both Time-Division Duplex (TDD) and Frequency-Division Duplex (FDD) modes.
- Scalable BW up to 20 MHz covering 1.4, 3, 5, 10, 15, and 20 MHz in the study phase.
- Increased spectral efficiency over Release 6 HSPA (High Speed Packet Access) by a factor of two to four.
- Reduced latency, to 10 ms RTTs between user equipment and the base station, and to less than 100 ms transition times from inactive to active.
- Self-optimizing capabilities under operator control and preferences that will automate network planning and will result in lower operator costs.

1.1.1 LTE Throughput Rates

The overall objective is to provide an extremely high-performance, radio-access technology that offers full vehicular speed mobility and that can readily coexist with HSPA and earlier networks. Because of scalable BW, operators will be able to easily migrate their networks and users from HSPA to LTE over time. Table 1.1 shows LTE peak data rates based on different DL and uplink designs [28]. Thus, Table 1.2 does a comparison of the peak data rate and peak spectrum efficiency between the different releases of LTE [27].

LTE is not only efficient for data but, because of a highly efficient uplink, is extremely efficient for Voice over IP (VoIP) traffic. In 10 MHz of spectrum, LTE VoIP capacity will reach almost 500 users

LTE Configuration	DL (Mbps) Peak Data Rate	UL (Mbps) Peak Data Rate
Using 2X2 MIMO in the DL and 16 QAM in the UL	172.8	57.6
Using 4X4 MIMO in the DL and 64 QAM in the UL	326.4	86.4

Table 1.1: LTE Peak Throughput Rate

		Rel. 8 LTE	LTE-Advanced	IMT-Advanced
Peak data rate	DL	300 Mbps	1 Gbps	1 Gbps (*)
	UL	75 Mbps	500 Mbps	
Peak spectrum efficiency [bps/Hz]	DL	15	30	15
	UL	3.75	15	6.75

Table 1.2: Peak data rate (1 Gbps data rate will be achieved by 4x4 MIMO and transmission bandwidth wider than 70 MHz approx.) and peak spectrum efficiency (*) 100 Mbps for high mobility and 1Gbps for low mobility

1.1.2 OFDMA and Scheduling

LTE implements OFDM in the DL. The basic principle of OFDM is to split a high-rate data stream into a number of parallel low-rate data streams, each a narrowband signal carried by a subcarrier. The different narrowband streams are generated in the frequency domain, and then combined to form the broadband stream using an Inverse Fast Fourier Transform (IFFT). In LTE, the subcarriers have 15 KHz spacing from each other. LTE maintains this spacing regardless of the overall channel BW, which simplifies radio design, especially in supporting radio channels of different widths. The number of subcarriers ranges from 72 in a 1.4 MHz channel to 1,200 in a 20 MHz channel.

The composite signal is obtained after the IFFT is extended by repeating the initial part of the signal (called the Cyclic Prefix (CP)). This extended signal represents an OFDM symbol. The CP is basically a guard time during which reflected signals will reach the receiver. It results in an almost complete elimination of multipath induced Intersymbol Interference (ISI), which otherwise makes extremely high data-rate transmissions problematic. The system is called orthogonal, because the subcarriers are generated in the frequency domain (making them inherently orthogonal), and the IFFT conserves that characteristic. OFDM systems may lose their orthogonal nature as a result of the Doppler shift induced by the speed of the transmitter or the receiver, this will be explained in detail in the Channel Implementation chapter where a Doppler filter is designed in order to simulate this phenomenon. 3GPP specifically selected the subcarrier spacing of 15 kHz to avoid any performance degradation in high-speed conditions. WiMAX systems that use a lower subcarrier spacing (~11 kHz) will be more impacted in high-speed conditions than LTE.

The multiple-access aspect of OFDMA comes from being able to assign different users different subcarriers over time. A minimum resource block (RB) that LTE can assign to a user transmission consists of 12 subcarriers over 14 symbols in 1.0 ms. Figure 1.2 shows how the system can assign these RBs to different users over both time and frequency.

By having control over which subcarriers are assigned in which sectors, LTE can easily control frequency reuse. By using all the subcarriers in each sector, the system would operate at a frequency reuse of 1; but by using a different one third of the subcarriers in each sector, the system achieves a looser frequency reuse of 1/3. The looser frequency reduces overall spectral efficiency, but delivers high peak rates to users at

the cell edge (having more interference from neighbour cells). Beyond controlling frequency reuse, frequency domain scheduling, as shown in Figure 1.3 [1] can use those RBs that are not faded, something that is not possible in CDMA-based systems. Since different frequencies may fade differently for different users, the system can allocate those frequencies for each user that result in the greatest throughput. This results in up to a 40% gain in average cell throughput for low user speed (3 km/hour), assuming a large number of users and no MIMO (Multiple Input Multiple Output). The benefit decreases at higher user speeds.

LTE is specified for a variety of MIMO configurations. On the DL, these include 2X2, 4X2 (four antennas at the base station), and 4X4. Initial deployment will likely be 2x2. 4X4 will be most likely used initially in femtocells. On the uplink, there are two possible approaches: single-user MIMO (SU-MIMO) and multi-user MIMO (MU-MIMO). SU-MIMO is more complex to implement as it requires two parallel radio transmit chains in the mobile device, whereas MU-MIMO does not require any additional implementation at the device. The first LTE release thus incorporates MU-MIMO with SU-MIMO deferred for the second LTE release.

LTE is designed to operate in channel BWs from 1.4 MHz to 20 MHz. The greatest efficiency, however, occurs with higher BW. The system, however, achieves nearly all of its efficiency with 5 MHz channels or wider.

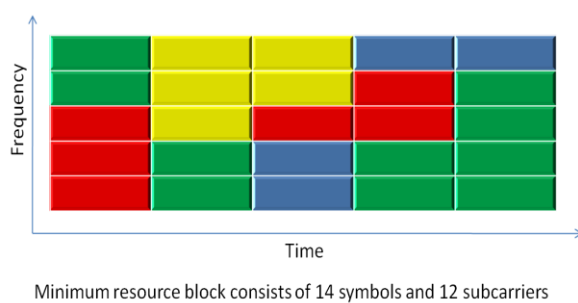


Figure 1.2: LTE OFDMA DL Resource Assignment in Time and Frequency

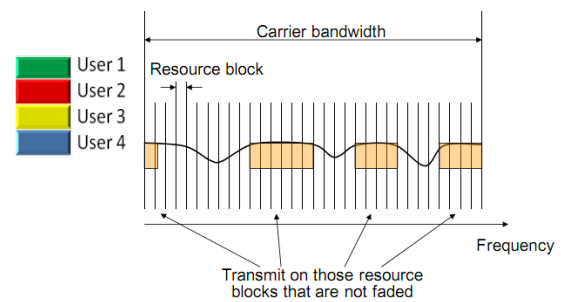


Figure 1.3: Frequency-Domain Scheduling in LTE

The previous features describe the radio interface which indeed is the context of this project. Regarding the core network of LTE, details are given in section A.1.4.1 from Annex A.

1.2 Problem statement

The objective of this project is to study the behaviour of the radio resource assignment in LTE under realistic conditions. It has been stated that scheduling is a key process in the functioning of the radio interface and two types of schedulers can be identified:

- Opportunistic: The scheduler considers the state of the radio channel in each RB in each user to make the best allocation possible of resources.
- Non-opportunistic: The allocation is blind, there is no knowledge of the channel state.

Obviously, the opportunistic option seems to be more interesting because it adapts to the radio channel conditions, on the other hand it requires a certain level of constant feedback from users informing about how the channel evolves along time. One of the objectives of this project is to evaluate the system performance under different degrees of feedback. Since a usual comparison is to assume complete and perfect channel

estimation, results will be presented in a comparative way. Different Channel Quality Indicator (CQI) reporting methods have been programmed and simulated. It is clear that a second objective is to program and simulate very realistically the LTE radio channel.

From the previous sections it is evident that LTE is a complex system with lots of interrelations among the elements that govern the network. Moreover, the system conditions evolve very quickly mainly due to:

- High level of burstiness in new data services.
- Wider BWs with frequency selective fading shared among users.
- The transmission time interval (TTI) is lower (1 ms) than in previous systems and resources can be scheduled to users as quickly as once every TTI.
- UEs mobility also contributes to this dynamism of the system. In fact, LTE should support even UEs in environments such as high speed trains where the radio channels shows the highest Doppler.

These constantly changing conditions imply that the analysis of the system performance cannot be addressed analytically. The methodology of this project is basically simulation, this allows to foresee the behaviour of the network under different deployment cases.

Traditionally, when assessing UMTS networks, system level simulators were mainly static. This means that they relied on MonteCarlo tests, in which a set of uncorrelated snapshots were independently generated and evaluated. In each snapshot, a set of users were randomly placed throughout the layout and the accumulation of results gave the probabilistic behaviour of the network. Because of the mentioned dynamism in the network conditions static simulations are not the best option for LTE.

WiComTec is a research group at UPC dealing with LTE radio aspects, among other topics. This PFC has been developed within this group and the starting point was an existent static LTE system level simulator, authored by the PhD. student David Gonzalez. Given the previous paragraphs to achieve the desired results one of the main tasks in this work has been to extend the simulation platform to allow it having more realistic results through dynamic simulations.

The development of a dynamic software requires many adaptations, such as introducing mobility to the users and updating their conditions accordingly, introduce several processes of the system such as Hybrid-ARQ with Incremental Redundancy [26] and the CQI reporting methods themselves, realistic consideration of the Reference Signals that are used in LTE to estimate the channel (see Chapter 4), etc. The new realistic radio channel model that has been programmed in the first stage of the project has also been introduced.

From here, the project has been structured in two well differentiated parts. Chapters 2 and 3 detail the strategies and the development of the LTE radio channel while chapter 4 explains the implementation of the dynamic LTE simulator, which results are presented in the last chapter.

CHAPTER 2. CHANNEL IMPLEMENTATION

This chapter is devoted to the realistic implementation of a radio channel in the context of dynamic LTE system level simulations. Initially, a study of the radio channel itself is presented along with the factors involved in its behaviour. Next, various approaches are compared and analysed in order to choose and implement the most appropriate and realistic one for the evaluation of LTE systems.

2.1 Radio channel phenomena

In communication systems the simplest channel is that just affected by a constant attenuation level and noise. This can be realistically modelled by adding white Gaussian noise (AWGN) to the attenuated signal and so the primary degradation source is the thermal noise and noise produced by the receiver. In radio channels more factors have to be taken into account: the attenuation given by the distance, the multipath propagation given by the reflections of paths or changes in the medium, and the shadowing given by objects (with large dimensions compared to the wavelength λ) situated between the transmitter and the receiver.

These phenomena are due to the heterogeneity and the constant changes in the radio channel medium, which can introduce power loss and distortion, caused by alterations in the environment which changes during time. These alterations, shown in figure 2.1 from [9], are due to: refraction (caused by the changes in the atmosphere composition and density and so in the refraction index), reflection (on floors, building, etc.), diffraction (due to objects cutting part of the wavefront, scattering (on any surface whose dimensions are in the order of λ or less) and abortion (caused by rain, snow, etc.).

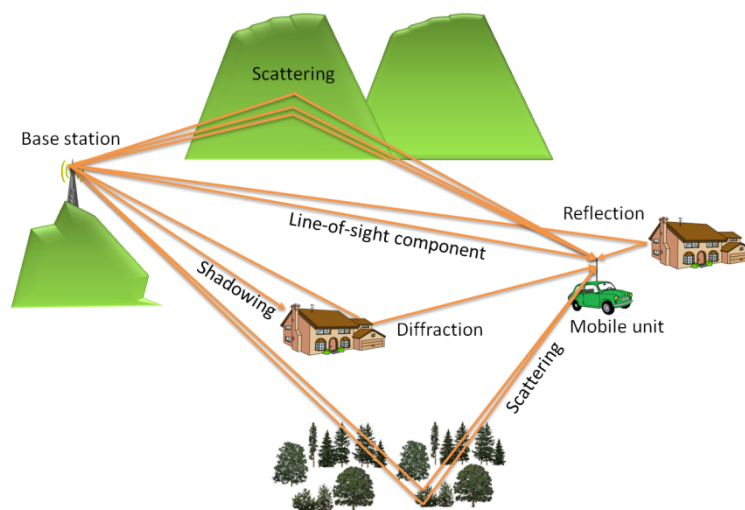


Figure 2.1: Example for a mobile radio scenario

As explained in [6], there are two types of fading effects that characterize mobile communications: large-scale and small-scale fading.

- Large-scale fading represents the average signal power attenuation or path loss due to motion over large areas and is commonly known as shadowing because it generates a radioelectrical shadow effect produced by prominent objects,

mainly terrain contours (e.g. hills, forests, buildings) in the context of mobile cellular networks. This effect can be realistically modelled by a log-normally distributed variation about the mean pathloss attenuation, this last term being due to the distance between transmitter and receiver.

- Small-scale fading refers to the dramatic changes in signal amplitude and phase that can be experienced as a result of small changes (as small as half a wavelength) in the spatial separation between a receiver and transmitter. Small-scale fading manifests itself in two mechanisms:
 - Frequency-spreading of the signal: Generated by the motion between the transmitter and receiver and that results in the appearance of Doppler effect and so a parasitic frequency modulation. If the multiple reflective paths are large in number and there is no line-of-sight signal component, the different Doppler frequencies and amplitudes of each paths implies that the envelope of the received signal is statistically described by a Rayleigh pdf. This time-variant manifestation of the fading can be categorized as fast- or slow-fading as explained in Section 1.1.
 - Time-spreading of the signal: Generated by the multiple paths in the radio signal. Depending on the symbol duration with respect to this delay spread, frequency selective fadings can appear and so signal distortion. This frequency-variant manifestation of the fading can be then categorized as frequency-selective or frequency-non-selective (flat), further explained in Section 1.2

The following sections focus on small-scale fading which is examined from the two domains that have been indicated: time and frequency.

2.1.1 Small-scale fading: Slow fading vs. fast fading

The distinction between slow and fast fading is important for the modelling of fading channels and for the performance evaluation of communication systems [8]. This time variant behaviour of the channel is due to motion (e.g. a receiver antenna on a moving platform).

A first characterization of this type of fading can be done with the so called coherence time T_c , which is the period of time over in which the channel impulse response is considered to be not varying and so its inverse gives an idea on the number of fadings per second. In other words this can be stated as the period of time after which the correlation function of two samples of the channel response taken at the same frequency but different time instants drops below a predetermined threshold (or more precisely as the time duration over which the channel's response to a sinusoid has a correlation greater than 0.5).

In the frequency domain this phenomenon is related to the frequency spread due to the Doppler effect, being f_d the maximum Doppler frequency possible. The f_d value depends on the speed of the mobile and the wavelength as shown in equation 2.1, and it is regarded as the typical fading rate of the channel, while T_c is the expected time duration over which the channel's response to a sinusoid is essentially invariant.

$$f_d = \frac{v_m}{\lambda} = \frac{v_m \cdot f_c}{c} \quad (2.1)$$

The Doppler spread is inversely proportional to the T_c . Equation 2.2 shows one of the approximations for the relation between the T_c and the Doppler frequency while equation 2.3 is the geometric mean of this expression and $1/f_d$ which is a popular rule used for this relation [6].

$$T_c \approx \frac{9}{16\pi f_d} \quad (2.2)$$

$$T_c \approx \sqrt{\frac{9}{16\pi f_d^2}} = \frac{0.423}{f_d} \quad (2.3)$$

Once the key factors involved in the time-variant manifestation are known, the next step is to describe when the channel defines a fast or slow fading:

- On the one hand, the terminology fast fading is used to describe a channel in which $T_s \gg T_c$ where T_s is the time duration of a transmission symbol, or similarly $B_s \ll f_d$ in the frequency domain, where B_s is the signal's bandwidth. In this case, several fades occur within a symbol time and so the signal waveform is dramatically distorted.
- On the other hand, slow fading is said to happen when $T_s \ll T_c$, and so $B_s \ll f_d$ in the frequency domain. In this case, symbols are just attenuated in a higher or lower level depending on whether they are transmitted during a deep fading or not.

2.1.2 Small-scale fading: Frequency-selective fading vs. flat fading

In a fading channel, the relationship between the excess delay time or Delay Spread D_s and the symbol rate T_s characterizes the signal dispersion, which is translated into frequency dependent fades in the frequency domain.

Depending on the relation between the coherence bandwidth B_c and the transmitted signal's bandwidth B_s the channel frequency response can be considered flat or selective. Note that B_c is defined as a statistical measure of the range of frequencies over which the channel passes all spectral components with approximately equal gain and linear phase. Thus, the coherence bandwidth represents a frequency range over which frequency components have a strong potential for amplitude correlation [10]. The D_s and the coherence bandwidth are related to channel multipath characteristics, differing for different propagation environments (such as, metropolitan areas, suburbs, hilly terrain, and indoors).

To characterize the dispersion introduced by the channel it is necessary to do an average of the powers from the different paths along time. The result is the Power Delay Profile (*PDP*) that can be expressed as a function of the delay τ :

$$P(\tau) = E_t \left\{ |\tilde{h}(\tau, t)|^2 \right\} \quad (2.4)$$

Given this, the D_s characterizes the average time spread of the channel. In particular, it is computed as the typical deviation of the *PDP* delay, shown in equation 2.5, being D the mean delay.

$$D_s = \sqrt{\int_{-\infty}^{+\infty} (\tau - D)^2 \cdot P(\tau) d\tau} \quad (2.5)$$

A universal relationship between coherence bandwidth and D_s that would be useful for all applications does not exist. An approximation can be derived from signal analysis (usually using Fourier transform techniques) of actual signal dispersion measurements in specific channels. In equation 2.6 an approximation is shown considering that the PDP is exponential, this is a typical situation where the first paths arrive with higher power and it descends exponentially with the other echoes. Thus given that:

$$P(\tau) = \frac{1}{D_s} e^{\frac{-\tau}{D_s}} u(\tau) \quad (2.6)$$

Then:

$$P(f) = \mathfrak{F}\{P(\tau)\} = \frac{1}{1+j2\pi f D_s} \Rightarrow B_c \cong \frac{1}{2\pi D_s} \quad (2.7)$$

The fading is flat when all the spectral components of the transmitted signal are affected in a similar manner. This applies for narrowband systems in which the BW of the transmitted signal is much smaller than the channel's coherence bandwidth. Using the factors described above:

- The channel has flat fading when $T_s \gg D_s$ in the time domain, or $B_s \ll B_c$ in the frequency domain.
- On the other hand, the fading is selective when the spectral components of the transmitted signal are affected by different amplitude gains and phase shifts. This is the case of wideband systems in which the transmitted BW is bigger than the channel's coherence bandwidth. So the channel is selective in frequency when $T_s \ll D_s$, or $B_s \gg B_c$ in the frequency domain.

2.1.3 LTE case: Frequency-selective but flat per subcarrier

The mobile standard of LTE uses OFDM technology which is a multi-carrier modulation that uses orthogonal waveform for modulating the sub-carriers. Since the sub-carriers are modulated by orthogonal waveforms, the sub-carriers are permitted to have overlapping spectrum, thus achieving higher spectrum efficiency and with the advantage of coping with severe channel conditions without complex equalization filters and high spectral efficiency.

In a simulator of OFDM, even though the whole signal assigned to a user can perceive frequency-selective fading, each subcarrier sees a flat channel due to its time duration is larger than the D_s . Notice that only the CPs already larger than the D_s . Thus the equalization in frequency is simple. A table of the LTE frequency bands is shown in section A.2 of Annex A.

LTE is a system with scalable BW. The width of a LTE carrier is defined by the concepts of Channel bandwidth (DBW) and Transmission bandwidth configuration (NRB) (see Figure 2.2). Their relation is shown in Table 2.1 obtained from [13].

Channel bandwidth $BW_{Channel}$ [MHz]	1.4	3	5	10	15	20
Transmission bandwidth configuration NRB	6	15	25	50	75	100

Table 2.1. Transmission bandwidth configuration NRB in LTE channel bandwidths

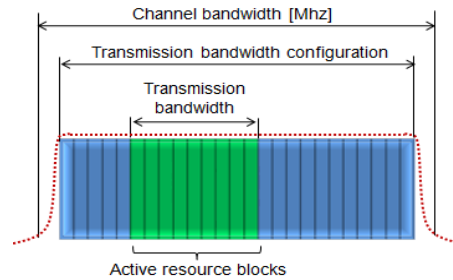


Figure 2.2: Definition of Channel Bandwidth and Transmission Bandwidth Configuration for one LTE carrier

NRB is defined as the maximum number of RBs that can be allocated within a LTE RF channel. A RB comprises 12 sub-carriers and can thus be understood to possess a nominal BW of 180 kHz. The physical layer specifications allow *NRB* to assume any value between 6 and 110, all RF requirements and thus a complete LTE specification are only defined for the values in the table This flexibility within the LTE specifications supports the addition of further options for transmission BW configurations (channel BWs), should the need arise.

Note from table 2.1 that the transmission BW configuration measures only 90% of the channel BW for 3, 5, 10, 15, and 20 MHz LTE and less so for 1.4 MHz LTE; e.g. for 5 MHz LTE a transmission BW of $25 \times 180 \text{ kHz} = 4.5 \text{ MHz}$ is obtained.

2.2 Necessity of channel simulation in a LTE system simulator

A channel simulation is very important in every communication system in order to evaluate its performance as well as to improve or optimize it by changing the system's parameters. So, in order to make the simulator useful it is necessary to make the channel simulation as realistic as possible, evaluating various methods and procedures to implement the most appropriate one for each case. Depending on the system level simulator, some fading components might not be necessary to be simulated, however for LTE, the simulation has to take into account all the phenomena introduced by the wireless communication.

2.2.1 Opportunistic scheduling in LTE

The process of scheduling is the one in which the radio resources are allocated depending on the user's conditions using CQIs. This forms parts of the Radio Resource Management which is executed in the eNodeB. Remember the process of scheduling in LTE is explained in section 1.1.4.2 of chapter 1.

It is important to simulate the channel over its frequency range and along time due to its time variance. These variations have to be accurately modelled since they have an important impact on opportunistic scheduling decisions. This type of schedulers are expected to be the most popular because they assign resources to users considering their particular channel conditions both in frequency and time, as it is graphically shown in figure 2.3.

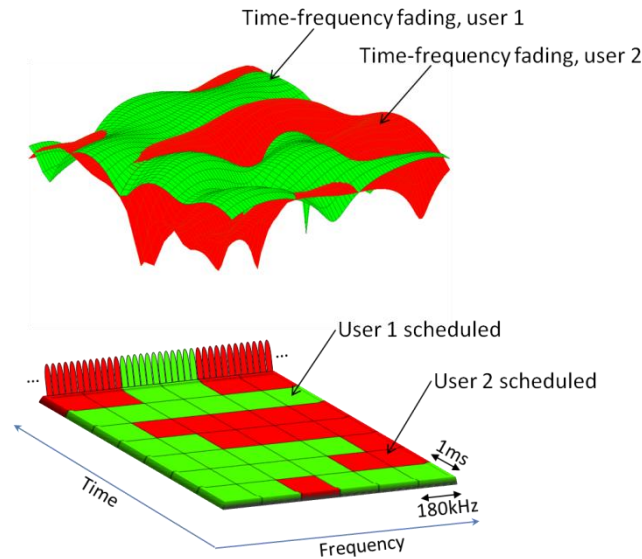


Figure 2.3: Example for LTE's channel-dependent scheduling in time and frequency domains

This graph shows the channel variations in two different users (red and green) and how the scheduler decides the best resources to assign to each one. Thus, at certain periods of time, some frequency ranges are better for the red user, and so the system decides to assign those groups of sub-carriers to this user. This is represented in the bottom part of the figure.

The available resources of each cell can be viewed as a two dimensional plane of time and frequency which can be seen in figure 2.4. In order to enable transmissions from and to users, the resource will be more finely divided so that each user is assigned certain frequency bands in certain subframes. Using OFDM transmission as a multiple access scheme by assigning different subcarriers to different users is referred to as OFDMA. The use of OFDMA means that the time-frequency resource can be seen as a grid, where each resource element corresponds to one OFDM subcarrier during one OFDM symbol time.

The main lobe BW of one subcarrier in LTE is $\Delta f = 15$ kHz meaning that the useful symbol time is $t_u = 1/\Delta f = 66.7$ μ s. The OFDM symbol time is the sum of t_u and the CP time t_{cp} (shown in figure 2.4). In order to fit seven symbols into one half of a subframe (one slot, 0.5 ms), t_{cp} is set to 5.2 μ s for the first symbol and to 4.7 μ s for the remaining six symbols. As mentioned above the smallest unit of resource that can be scheduled is a RB and is made up of 12 subcarriers during one subframe, i.e. $12 \cdot 7 \cdot 2 = 168$ resource elements. The BW of LTE is easily scalable and can vary from 6 RBs (1 MHz) to more than 100 RBs (20 MHz).

The time axis is split up into 10 ms long frames, each divided into 10 subframes.

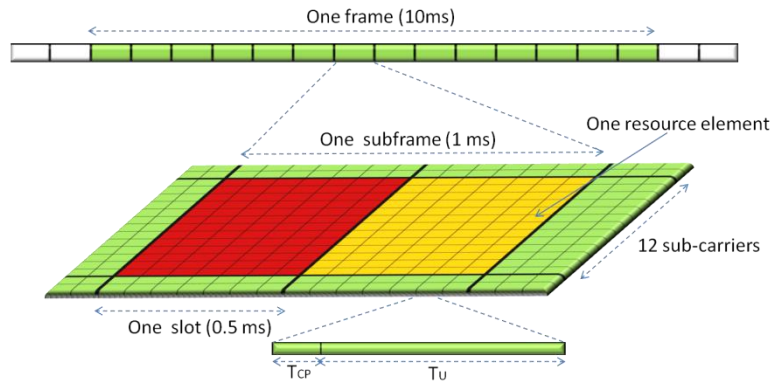


Figure 2.4: LTE's resource grid

2.2.2 Channel state information for scheduling and link adaptation

In LTE there are three indicators that reflect the Channel State Information (CSI): Rank Indicator (RI), Precoding Matrix (PMI) and CQI. Whereas the first two ones are used for MIMO (Multiple Input Multiple Output) operation, the CQI is the most important one from a scheduling and link adaptation viewpoint.

The CQI helps the eNodeB to select the modulation scheme and code rate (Adaptive Modulation and Coding, AMC) depending on a prediction of the DL channel conditions. As said in [13], it does it by providing the eNodeB information about the link status and the parameters (modulations and codes) the user's equipment UE can handle. The CQI is a value from a table containing 16 possible entries, which can be seen in table 2.2, with Modulation and Coding Schemes (MCSs). A simple method by which a UE can choose an appropriate CQI value could be based on a set of Block Error Rate (BLER) thresholds. The UE would report the CQI value corresponding to the MCS that ensures $BLER \leq 10\%$ based on the measured received signal quality.

CQI index	Modulation	Coding rate x 1024	Bits per resource Element
0	out of range	-	-
1	QPSK	78	0.1523
2	QPSK	120	0.2344
3	QPSK	193	0.3770
4	QPSK	308	0.6016
5	QPSK	449	0.8770
6	QPSK	602	1.1758
7	16QAM	378	1.4766
8	16QAM	490	1.9141
9	16QAM	616	2.4063
10	64QAM	466	2.7305
11	64QAM	567	3.3223
12	64QAM	666	3.9023
13	64QAM	772	4.5234
14	64QAM	873	5.1152
15	64QAM	948	5.5547

Table 2.2: CQI table [13]

Hence, the UE has to report the eNodeB with this channel feedback, which the eNodeB will use as extra information, the final AMC does not need to follow the configuration in the table. In LTE the channel feedback reporting is always fully controlled by the eNodeB and the UE cannot send any channel state feedback reports without eNodeB knowing it beforehand. A simple representation of this communication is done in figure 2.5

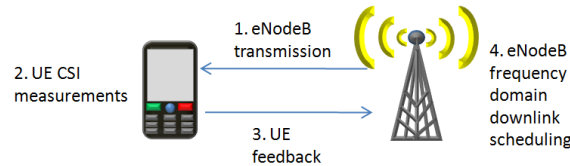


Figure 2.5: Channel State Information (CSI) reporting procedure

One of the most usual assumptions when simulating LTE systems is that the time between the user link measurement, the reporting and the final resources allocation by the eNodeB takes place in a time much lower than the coherence time. However, this is just true for users with slow motion. In particular, figure 2.6 shows the reporting architecture in a more detailed manner, indicating the required time in each step [C]. From here, an estimated total time of X ms is obtained which corresponds to the T_c of a user moving at Y km/h, if the user moves at a speed of this order or higher, the information being used by the eNodeB to allocate resources will be outdated and so the scheduling will not operate at its best.

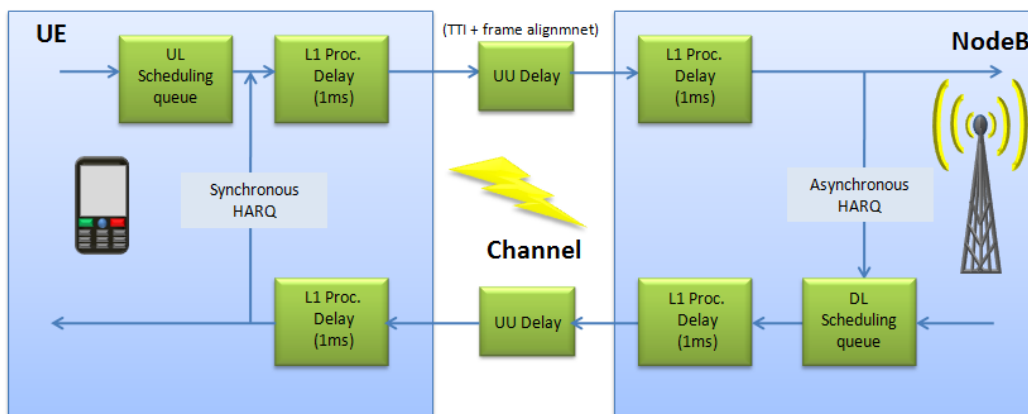


Figure 2.6: Channel State Information (CSI) reporting procedure. Delays

From a system level simulation viewpoint, it is important to include a precise and correlated channel variation so that effects derived from this “outdated information” can be modelled realistically.

Regarding frequency, as the channel is flat per sub-carrier, it is enough to simulate one point per sub-carrier will be obtained. Nevertheless, notice that the exact frequency response of all the BW has to be simulated in order to take into account the frequency correlation between adjacent sub-carriers in the radio blocks assigned by the scheduler. The procedure will be as follows:

- 1- Generate the channel
- 2- Extract the frequency response
- 3- Assign a gain to each sub-carrier

4- Repeat the procedure en each time-step

Depending on the resolution of the time step in the simulation and the T_c of simulated users, in some cases temporal correlation will not be required (fast users with relatively large time steps). In those cases, each realization of the channel will be generated randomly independent. This can be further understood by looking at figure 2.7.

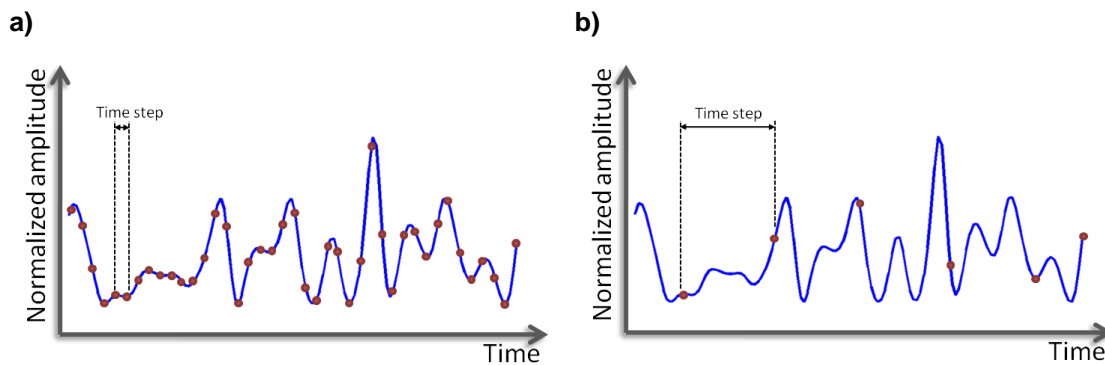


Figure 2.7: Evolution in time of the fast fading channel. **a)** Small time step, **b)** Large time step

2.3 Channel simulation strategies

There are various methods and strategies in order to simulate the wireless channel. This section constitutes a brief overview of them, analysing the advantages and drawbacks in order to select the most appropriate one for the specific simulation of LTE systems.

2.3.1 Sum-of-Sinusoids Simulators

One of the techniques used to model fading signals due to multipath is the sum-of-sinusoids (SoS). This method was initially proposed by Jakes [19], but as indicated in [3], SoS methods have been proposed for fading channel simulation over the past three decades.

The rationale behind this approach is to create a fading process by superposing several waves, each one being characterized by amplitude, an angle of arrival, and a phase just as in Clarke's physical model. Some of the more popular methods are:

- The deterministic simulation model, in which all parameters of the simulation (amplitudes, angles of arrivals, and phases) are deterministic quantities: hence the same fading waveform is reproduced for every trial run of a simulation; and
- The stochastic simulation model in which at least one parameter is a random quantity.

As an advantage just point out that the SoS method generates the fading process sample-by sample, hence there is no significant delay in the simulation. One of the drawbacks is that to obtain a satisfactory accuracy, several tens (or hundreds) of sinusoids usually need to be generated in the SoS method, which is computationally cumbersome (although some fast SoS simulators based on a lookup table approach can be devised). Another problem is that many methods do not generate a stationary and ergodic stochastic process, thus losing realism.

Even though the SoS methods are still present in the current scientific literature, the development of Filtered Gaussian Noise (FGN) Simulators allow more flexibility in the specification of the Doppler spectrum. The next section explains this method as well as it presents its advantages and drawback compared with the SoS method.

2.3.2 Filtered Gaussian Noise Simulators

A complex Gaussian fading process with desired spectral properties can be directly simulated by generating a complex Gaussian process and filtering it with a Doppler filter. The Doppler filter should be designed to produce the desired Doppler spectrum.

The Complex Gaussian random sequences employed in this project are designed to have mean zero and variance one in the frequency domain. Thus, each sequence corresponds to a modelled ray, which will be modelled according to the ITU power delay profiles of an ITU channel model, per example Pedestrian B or Vehicular A.

The filtering operation can be done in the time domain or the frequency domain:

- In the time domain the simulator must perform (in the case of finite impulse response (FIR) filters) a direct linear convolution of the generated complex Gaussian process with the impulse response of the Doppler filter.
- In the frequency-domain the Gaussian process spectrum is multiplied with the filter's frequency response. This speeds up simulation for large blocks of samples to be generated, but inherently requires samples to be produced as blocks, which can introduce larger delays and consume more memory.

An advantage of the FGN in front of SoS is that this method allows any arbitrary Doppler spectrum to be specified, as long as the Doppler filter impulse response has enough coefficients. Note then that for very small fading rates, long impulse responses may be needed. Another advantage of this approach is that it only requires filtering to be performed, for which many computational efficient approaches exist. Unlike SoS, the FGN method does require a block of input samples to be available (especially and as just explained, if frequency-domain filtering is used), hence the drawback is that some delay is introduced: however the size of the block of samples can be adjusted.

In a system level simulator the number of operations to perform is huge and that is why it is preferable to compute the wireless channel prior to simulations. So, processing time has been preferred to memory requirements because the global behaviour of the channel, both in time and frequency, is loaded in memory at the beginning of each simulation. Given this, the chosen method in this project is the FGN.

The next step is to study the two filtering operations in order to decide if it is more appropriate to filter in time or in frequency.

2.3.2.1 Time filtering. Jakes Doppler Spectrum

The purpose of the Doppler filter is to shape the generated complex Gaussian noise process such that the filtered process has the desired Doppler power spectrum. There are several common power spectrum models for fading processes: Jakes Doppler Spectrum, Flat Doppler Spectrum, Gaussian Doppler Spectrum, Symmetrical

Restricted Jakes Doppler Spectrum, Asymmetrical Jakes Doppler Spectrum, Bi-gaussian Doppler Spectrum and Rounded Doppler Spectrum among others. In this study it has been decided to use Jakes Doppler Spectrum because it is the generic model, commonly named “classical model” and it suits with our simulation environment. Another option such as the Flat Doppler Spectrum is suitable for 3-D isotropic scattering evaluations, or the Gaussian Doppler spectrum which is a good model for multipath components with long delays in Ultra High Frequencies (UHF) communications.

The Jakes Doppler Spectrum applied to a mobile receiver considers the following acceptable assumptions:

- The radio waves propagate horizontally.
- At the receiver, the angles of arrival of the radio waves are uniformly distributed over $[-\pi; \pi]$.
- At the receiver, the antenna is omnidirectional, i.e. the antenna pattern is circular-symmetrical.

The baseband normalized Jakes Doppler spectrum is given analytically by:

$$S_j(f) = \frac{1}{\pi f_d \sqrt{1-(f/f_d)^2}}, |f| \leq f_d \quad (2.8)$$

Where f_d is the maximum Doppler shift. The corresponding autocorrelation is:

$$R_j = J_0(2\pi f_d \tau) \quad (2.9)$$

Where $J_0(z)$ is the Bessel function of the first kind of order 0. The amplitude of the frequency response is then given by $|H_j(f)| = \sqrt{S_j(f)}$ and the impulse response can be derived as:

$$h_j(t) = \Gamma(3/4) \left(\frac{f_d}{\pi|t|} \right)^{1/4} J_{1/4}(2\pi f_d |t|) \quad (2.10)$$

Where $\Gamma(\cdot)$ is the gamma function. The value of $h_j(t)$ at $t = 0$ is calculated as $\lim_{t \rightarrow \infty} h_j(t)$. The discrete-time impulse response used for simulation is a sampled, truncated (to M points), causal (delayed by M/2 points) version of $h_j(t)$, given by:

$$h_j[m] = h_j(t = (m - M/2)t_s) = \Gamma(3/4) \left(\frac{f_d}{\pi|(m - M/2)t_s|} \right)^{1/4} J_{1/4}(2\pi f_d |(m - M/2)t_s|) \quad (2.11)$$

For $m=0, 1, \dots, M-1$.

Notice that equation 2.11 gives an infinite value for $m=M/2$. To solve this problem it is necessary to calculate the limit $\lim_{m \rightarrow M/2} h_j[m]$ at this point.

In order to filter in time, there are two ways to develop the Doppler filter, by generating it directly in time using equation 2.10 or by generating the frequency response from equation 2.8 and then do the IFFT. In the following subsections an analysis of both will be done by showing the simulation results done in MATLAB and comparing the advantages and drawbacks.

2.3.2.1.1 Generation of the filter in time

As mentioned above, this section implements Doppler's filter impulse response using equation 2.10, specifically the truncated causal version given by equation 2.12. Figure 2.8 shows an example of Jake's Doppler filter. In this example the filter is done with 128 points, $f_d=6\text{Hz}$ and $f_s=100\text{Hz}$.

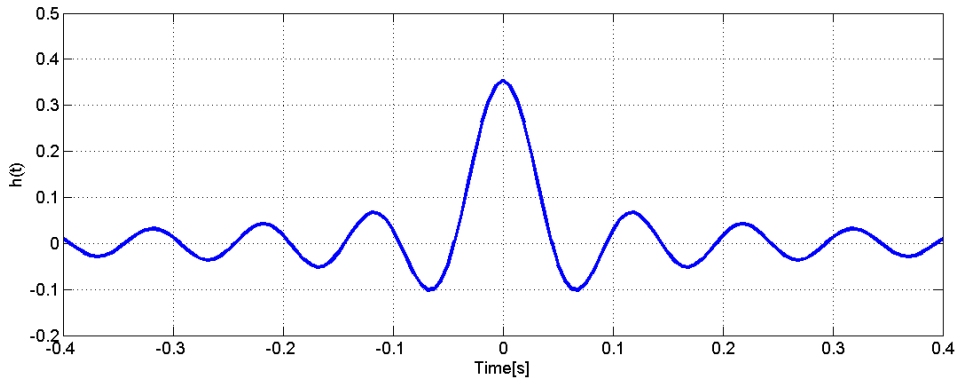


Figure 2.8: Jake's Doppler filter. 128 points, $f_d=10\text{Hz}$, $f_s=160\text{Hz}$

As the filter impulse response has been windowed by a rectangular pulse in the time domain, by doing the Fourier transform it becomes infinite in frequency. The discrete Fourier transform (DFT), or fast Fourier transform (FFT) in this case, replicates the Fourier transform in 0 and $N-1$ (in the discrete-time Fourier transform (DTFT) it is 2π), so the two replicas overlap between 0 and $N-1$ (2047), leading to aliasing. The direct DFT equation is shown in equation 2.12.

The result of doing a 2048-point FFT of $h_j[n]$ is shown in figure 2.9. The figure is limited to such frequencies that the gain changes between $-f_d$ and f_d are best represented. However, the complete 2048 points are plotted next to it. Due to the sum of alias, the difference between the highest point and the point in zero is smaller than it should be (approx. 2.91 dB). This can be better appreciated if it is compared with figure 2.10 which is the ideal frequency response. As mentioned above, $N-1$ corresponds with 2π in the DTFT, and as the frequency response is the one represented, $N-1$ corresponds with the sampling frequency which is $\Delta f \cdot n_{FFT} = 30.72 \text{ MHz}$, being $\Delta f = 15 \text{ kHz}$ as mentioned in section two of this chapter, and $n_{FFT} = 2048$ as defined above.

The solution to the aliasing problem is to increase the sampling frequency, which yields to an increase in the computational complexity: a) When generating the filter and b) when performing the filtering process.

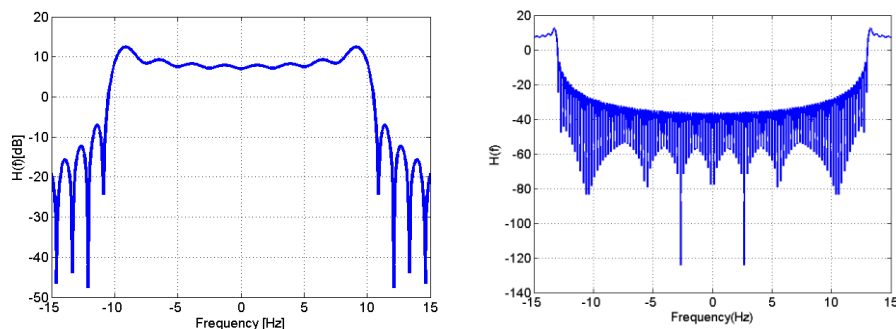


Figure 2.9: Jake's Doppler filter frequency response. 2048-point FFT, $f_d=10\text{Hz}$

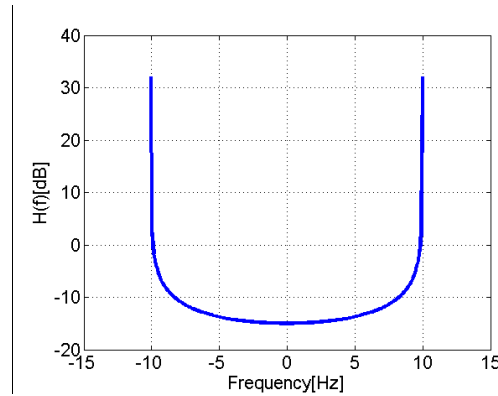


Figure 2.10: Jake's Theoretical Doppler filter frequency response. 385 points, $f_d=10\text{Hz}$, $f_s=160\text{Hz}$

The direct DFT formula is show in equation 2.12 and the inverse DFT in equation 2.13. The FFT is a 2^n -point DFT which is easier to compute.

$$X_k = \sum_{n=0}^{N-1} x_n e^{-\frac{2\pi i}{N}kn} \quad k=0, \dots, N-1 \quad (2.12)$$

$$x_n = \frac{1}{N} \sum_{k=0}^{N-1} X_k e^{-\frac{2\pi i}{N}kn} \quad n=0, \dots, N-1 \quad (2.13)$$

2.3.2.1.2 Generation of the filter in frequency

In the case of generating the filter in frequency, the idea is to implement equation 2.8, shown in figure 2.10, and then transform it into the time domain with the IFFT from equation 2.13.

In order to do this, the number of points in which the IFFT is computed is limited and so the signal is being implicitly windowed. This is equivalent to a circular convolution with the IFFT of the window and so temporal aliasing appears.

The aliasing effect can be appreciated by comparing figure 2.11 with figure 2.8 and noticing that the difference between the main lobe and the side lobes is greater in figure 2.11 due to the sum of alias.

Even if the convolved signal in the filtering is $h(t)$, figure 2.12 shows the FFT of the created impulse response. Notice the difference with figure 2.9, in this case there is less aliasing in frequency, the difference between the highest point and the point in zero frequency is approximately 18.78 dB (aprox. 15.87 dB more that before).

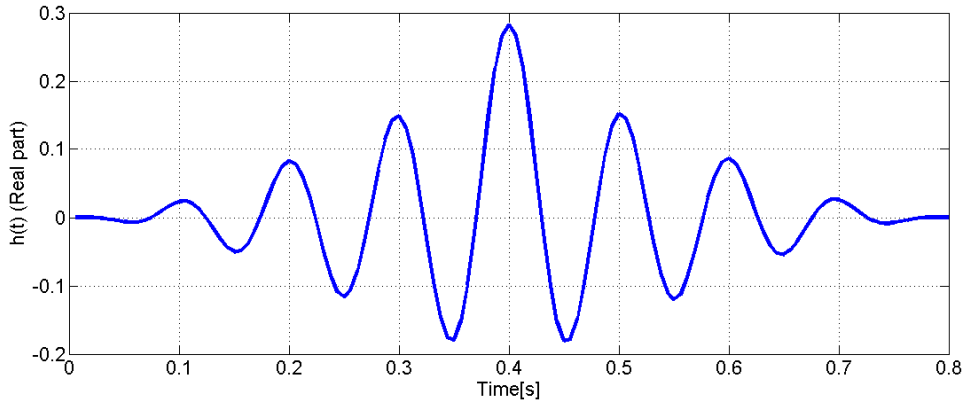


Figure 2.11: Jake's Doppler filter. 128 points, $f_d=10\text{Hz}$, $f_s=160\text{Hz}$

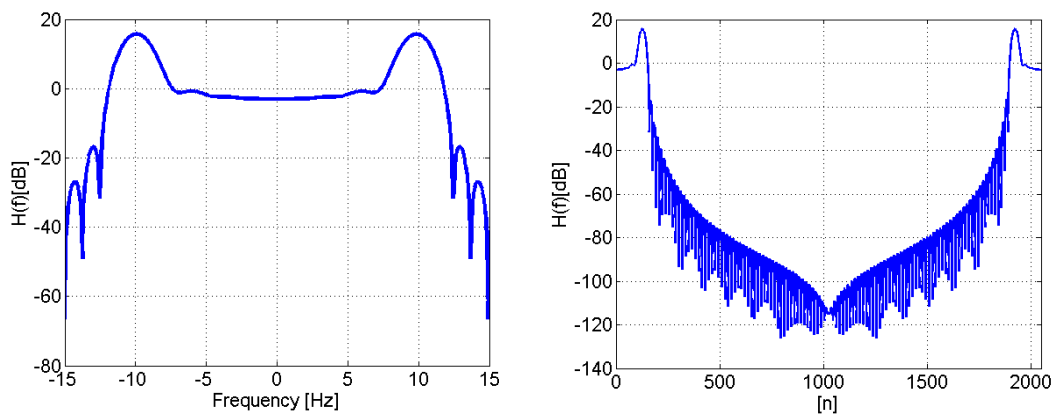


Figure 2.12: Jake's Doppler filter frequency response. 2048-point FFT, $f_d=10\text{Hz}$, $f_s=30,72\text{MHz}$

2.3.2.2 Frequency filtering. Young's and Bealieu's IDFT Model

This model obtained from [7] does the filtering directly in frequency by multiplying the real and complex part of a zero-mean Gaussian stochastic process with a certain filter, also created in the frequency domain. In the method, the inverse discrete Fourier transform (IDFT) operation is applied to complex sequences of independent, normally distributed random numbers, each sequence weighted by appropriate filter coefficients. Figure 2.13 represents the block diagram of the algorithm. The technique was proposed by Smith and requires multiplying 4 sequences and executing an N-point complex inverse DFT twice, so computationally is rather demanding.

The desired algorithm output is a Rayleigh-distributed sequence with specified correlation properties. Generation of the in-phase component of the fading process is represented by the upper half of the diagram, generation of the quadrature component is identical and represented by the lower half. In each case, the algorithm starts with two independent sequences of independent and identically distributed (i.i.d.) random variables with a normal distribution, zero mean and variance σ^2 .

The sequences are weighted by appropriate filter coefficients $\{F[k]\}$, and added in quadrature to form the complex Gaussian sequence $\{X[k]\}$. An IDFT is then taken of this complex sequence to form complex time samples, which for the in-phase branch will here be denoted $\{x^{(1)}[n]\}$. Then, the real part $\text{Re}\{x^{(1)}[n]\}$, is added in quadrature with the real part from a second identical and independent branch, $\text{Re}\{x^{(2)}[n]\}$, producing

complex samples which model the fading channel accurately. The imaginary parts of each sequence are discarded because they are correlated with the real ones. Indeed this is the reason that leads the algorithm to need four different Gaussian sequences

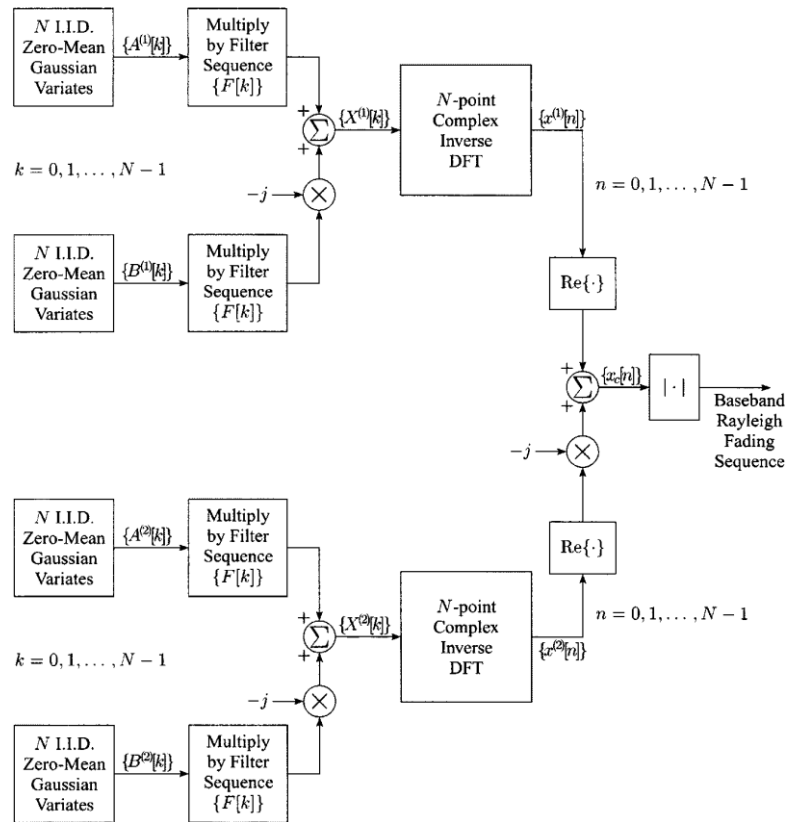


Figure 2.13: Block diagram of the algorithms of Smith to generate correlated Rayleigh variables from [7]

Young and Bealieu proposed a modification of the algorithm in [7] to reduce the required computational resources. They intelligently modified the values in $F[k]$ to generate statistically identical samples with only two products and a single IDFT operation.

As mentioned before, it is necessary to have independence between the real and imaginary parts of the complex Gaussian sequence used to form the Rayleigh process. But the complex output sequence from a single IDFT step does not have this property, so two such sequences must be formed independently, and the imaginary part of each sequence discarded. Hence, the output of a single IDFT can be used directly, by properly modifying the filter coefficients. The resulting block diagram is shown in figure 2.14.

The modified filter $F_M[k]$ enabling the use of a single IDFT is given by equation 2.15.

$$F[k] = \begin{cases} 0, & k = 0 \\ \sqrt{\frac{1}{2\sqrt{1-\left(\frac{k}{Nf_m}\right)^2}}}, & k = 1, 2, \dots, k_m - 1 \\ \sqrt{\frac{k_m}{2} \left[\frac{\pi}{2} - \arctan\left(\frac{k_m-1}{\sqrt{2k_m-1}}\right) \right]}, & k = k_m \\ 0, & k = k_m + 1, \dots, N - k_m - 1 \\ \sqrt{\frac{k_m}{2} \left[\frac{\pi}{2} - \arctan\left(\frac{k_m-1}{\sqrt{2k_m-1}}\right) \right]}, & k = N - k_m \\ \sqrt{\frac{1}{2\sqrt{1-\left(\frac{N-k}{Nf_m}\right)^2}}}, & k = N - k_m + 1, \dots, N - 2, N - 1 \end{cases} \quad (2.14)$$

Where k_m is an index which defines the point at, or just below, the maximum Doppler frequency, shown in equation 2.15.

$$k_m = \left\lfloor f_d \left(\frac{f_s}{N}\right)^{-1} \right\rfloor = \lfloor f_m N \rfloor \quad (2.15)$$

And $f_m = f_d/f_s$ is the maximum Doppler frequency normalized by the sampling rate.

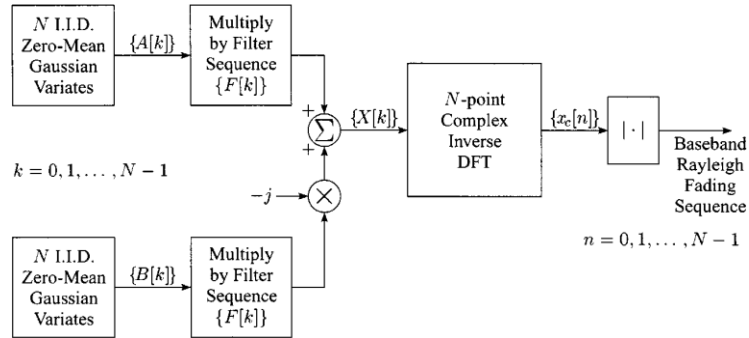


Figure 2.14: Block diagram of the improved algorithm using a single complex IDFT to generate correlated Rayleigh variables

As mentioned in [15], computationally this approach is quite efficient, since the heaviest effort is required by the IFFT, which only costs $O(N \log N)$ operations, where N is the number of time-domain sampled Rayleigh channel coefficients.

2.3.2.3 Auto-regressive filter

The Auto-regressive (AR) filter model imposes an all-pole structure on the filter $H(f)$ and determines the AR filter coefficients in the time-domain by using the knowledge of the channel auto-correlation function. However, it must be noted that the underlying principle of filtering Gaussian noise to produce an output with the desired power spectral density (pds) remains the same [14].

Let $x(n)$ be a white, Gaussian random process filtered through a p^{th} order (p poles) AR filter, that is a filter whose z transform is given by:

$$H(z) = \frac{1}{A_p(z)} = 1/(1 + \sum_{k=1}^p a_p(k)z^{-1}) \quad (2.16)$$

Then, the output $y(n)$ is given by the following equation.

$$y(n) = -\sum_{k=1}^p a_p(k)x(n-k) + x(n) \quad (2.17)$$

If the auto-correlation, $r_{yy}(n)$, of $y(n)$ is known for the delays ranging from $n = 0$ to $n = p$, the filter coefficients a_p can be chosen to exactly reproduce these auto-correlation values in the output signal $y(n)$. The necessary filter coefficients obey the Yule-Walker equation.

$$\begin{pmatrix} r_{yy}(0) & \cdots & r_{yy}(p-1) \\ \vdots & \ddots & \vdots \\ r_{yy}(p-1) & \cdots & r_{yy}(0) \end{pmatrix} \begin{pmatrix} a_p(1) \\ a_p(2) \\ a_p(3) \\ \vdots \\ a_p(p) \end{pmatrix} = -\begin{pmatrix} r_{yy}(1) \\ r_{yy}(2) \\ \vdots \\ r_{yy}(p) \end{pmatrix} \quad (2.18)$$

Which can be written in the matrix form as $R_{yy}a_p = -r$ and $a_p = -R_{yy}^{-1}r$.

However, an exact solution to the Yule-Walker equation does not exist if the auto-correlation matrix R_{yy} is singular and therefore non-invertible. In such cases, a solution is obtained by using a technique called "diagonal loading" or "matrix stabilization", where some noise variance is artificially introduced into R_{yy} to make it stable, non-singular and thus invertible matrix. The a_p values are obtained as shown in equation 2.19.

$$a_p = -(R_{yy} + \epsilon I)^{-1}r \quad (2.19)$$

Where I is a $p \times p$ identity matrix and $\epsilon \neq 0$ is a suitable diagonal loading parameter that renders $(R_{yy} + \epsilon I)$ non-singular and invertible.

This approach is discarded due to the filter design requires high orders to approximate well the autocorrelation at large lags [15].

2.3.3 Chosen and implemented filter

Once the various approaches have been studied, the next step is to choose the most appropriate one for the simulation of LTE systems. Along the different explanations, some methods have been discarded, now a brief summary of the disadvantages is done.

To begin with, the SoS method is discarded because the FGN's allows more flexibility in the specification of the Doppler spectra and less computational cost for large volumes of data to be assessed. As mentioned above, this method has two approaches, the generation of the filter in frequency or in time. Both have been simulated and discarded due to the problem of aliasing. The last method explained has been the AR filter, ruled of due to the filter design requires high orders. Hence the chosen filter has been Young's and Bealieu's IDFT model.

Following the block diagram of figure 2.14, once created the zero-mean Gaussian variables and multiplied by the filter's response $F[k]$ at each branch (real and imaginary), $X[k]$ is the complex result of the sum of these branches. Figure 2.15 shows $X[k]$ along k and the taps.

Then, the N-point Complex Inverse DFT of $X[k]$ is $xc[n]$, which in this case is a 128-point FFT. Figure 2.16 shows the evolution in time of $xc[n]$ for each delay.

Now, once obtained the baseband Rayleigh's fading sequence the next step is to do a FFT in order to view the fadings for each frequency along time. Notice that in figure 2.17 the frequency response is normalized and truncated to the useful LTE's BW. It can be clearly appreciated how the signal evolves in frequency and time. Given this 18 MHz BW, the channel will be frequency selective for usual macrocellular delay spreads (100 ns to 10 μ s), however recall that at sub-carrier level it is flat.

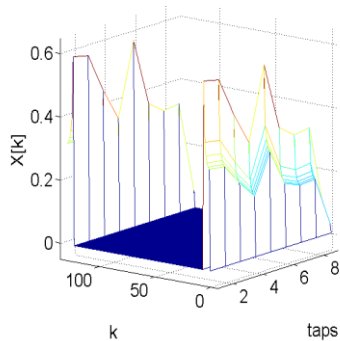


Figure 2.15: $X[k]$ from figure 2.13

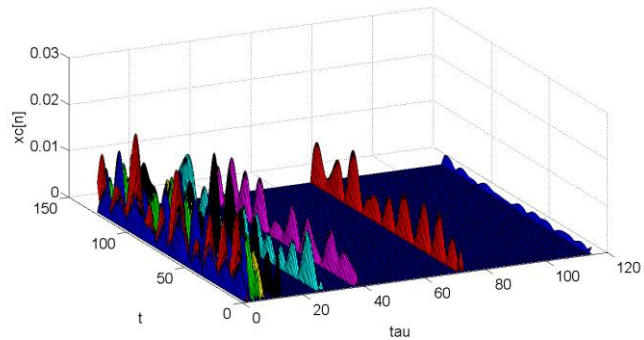


Figure 2.16: $xc[n]$ from figure 2.14. (N-point Complex Inverse DFT of $X[k]$)

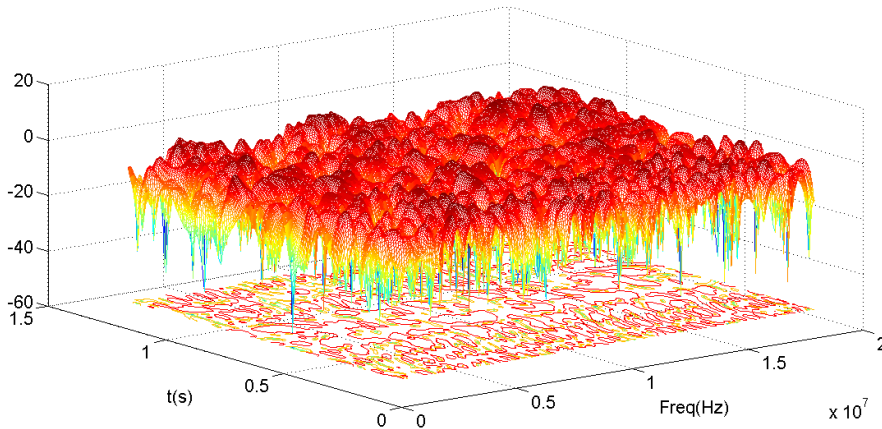


Figure 2.17: Channel's frequency response along time

CHAPTER 3. SIMULATOR

As mentioned in the problem statement, the objective of this project is to study the behaviour of the radio resource allocation in LTE under realistic conditions (see chapter 4). In order to accomplish this objective a realistic LTE radio channel must be developed. To achieve this, an extra module has been applied to the existing system simulator, in concrete a channel simulator module has been programmed in C++ implementing the approach detailed in chapter 2. This chapter aims to explain the main parts of the new module and also explains in detail the modifications done to the resulting channel in order to load it in the dynamic LTE simulator.

3.1 C++ Channel Simulator application introduction

The developed program is separated in two main parts, the system simulator, where the simulations are done, and the additional scripts where other additional parameters are studied. Figure 3.1 shows the main window of the simulator's Graphical user interface (GUI). Button (1) of figure 3.1 gives access to the system simulator's main panel which is explained in section 3.2.2. When the tab named "Additional scripts" is selected, the panel shown in figure 3.2 will appear. The channel simulator, shown in figure 3.3, is accessed by (7) in the additional script tab. Further explications of how the simulator works are done in the following subsections.

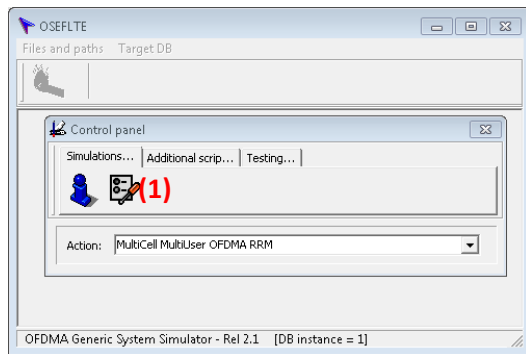


Figure 3.1: System simulator's main window

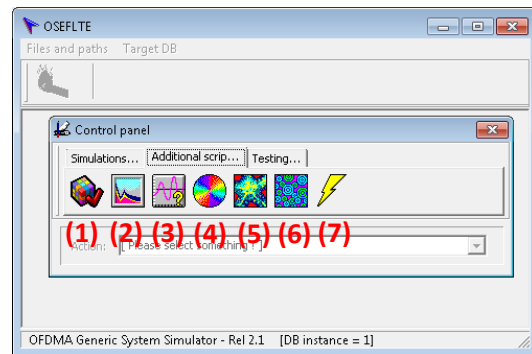


Figure 3.2: System simulator's Additional Script window

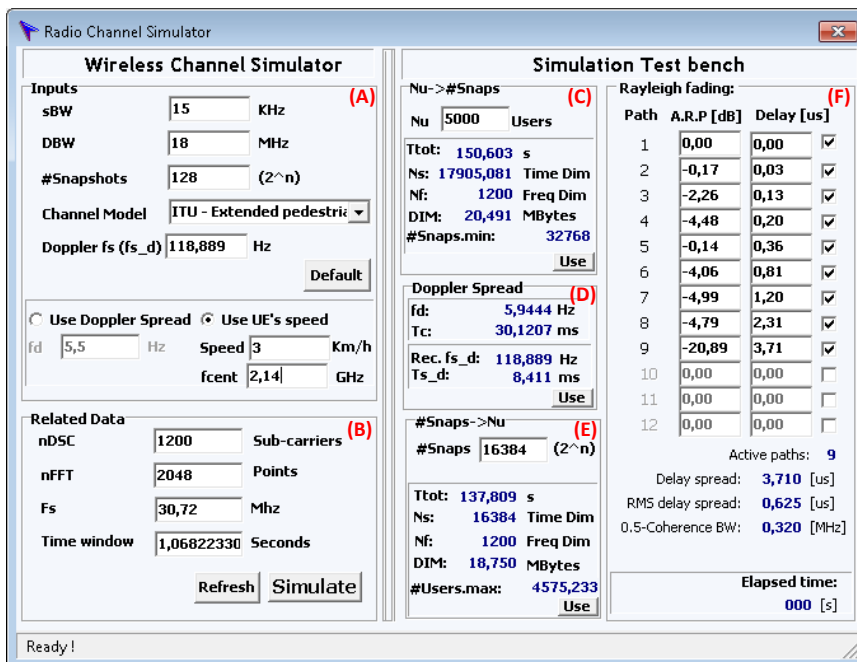


Figure 3.3: Wireless Channel Simulator application

3.2 Channel simulator

As mentioned above, the channel simulator has been implemented as one of the Additional Scripts in the LTE simulator. So, the channel is created, saved in binary files, and loaded in the system simulator. The procedure followed to obtain the results of the simulations is represented in the diagram of figure 3.4. This section is focused in the wireless channel simulation, for information about the system simulator see chapters 4 and 5.

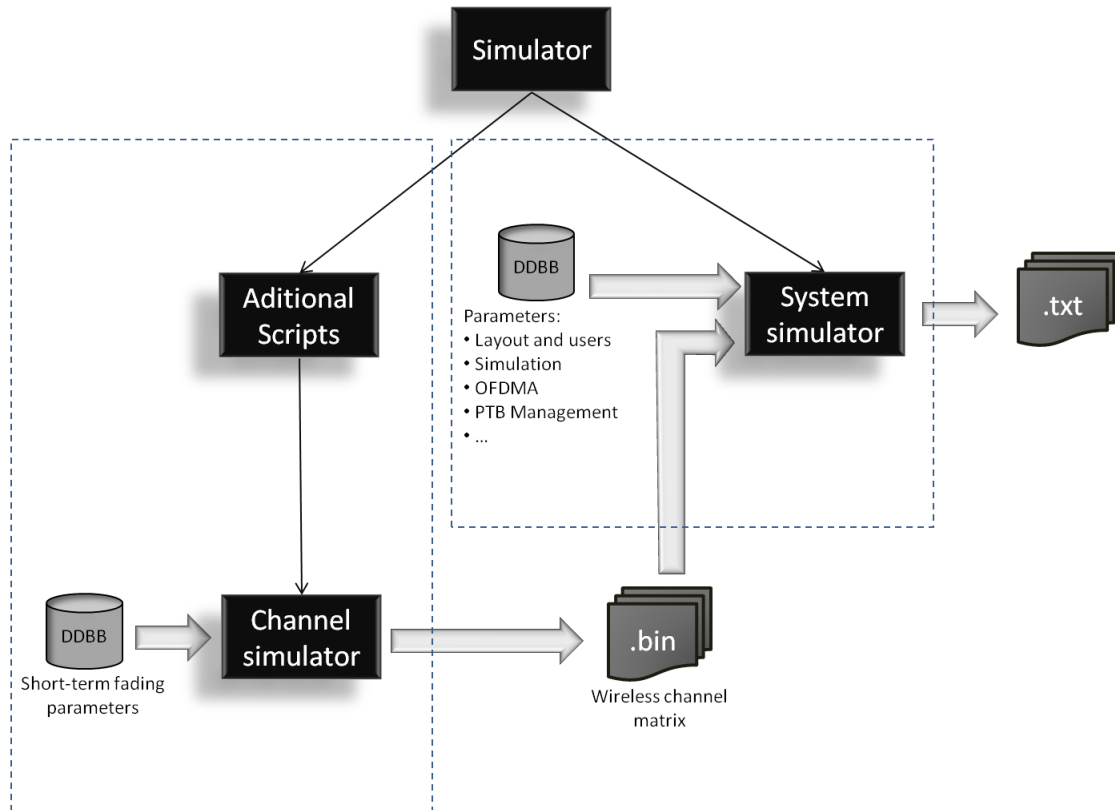


Figure 3.4: Simulator's basic block diagram

The channel simulator application is organized in two parts: the simulation section named Wireless Channel Simulator and the test section named Simulation Test Bench. On the one hand, the test section is used to evaluate the relationship between the channel simulator and the system simulator, as well as to obtain certain related data. The top and the bottom subsections, (C) and (E) of figure 3.3, are used to obtain the minimum number of snapshots to be able to simulate the desired number of users, as well as to obtain the maximum number of snapshots for a certain number of users. The constrain applied to obtain this, is that statically, they have a temporal separation equal to a coherence time. The centre section (D) of figure 3.3, shows the Doppler frequency, the T_c and the recommended Doppler sampling frequency, related to the speed and the centre frequency introduced in the input section. On the right side, in (F), depending on the selected channel model it shows the characteristics of the power delay profile, which is the average power and delay for the different paths.

On the other hand, the simulation section is composed by the inputs (A) and the related data necessary to simulate the wireless channel (B). The inputs are the following:

- *sBW* (OFDM sub-carrier spacing): In the LTE case this must be adjusted to be 15 kHz. This value is used to calculate the number of data sub-carriers (nDSC)

as well as the sampling frequency, because when creating the frequency response of the radio channel, there is one sample per subcarrier.

- *DBW*: the total BW chosen for this project is 20 MHz, but taking into account the guard bands, the useful BW becomes 18 MHz. With this configuration, the total number of sub-carriers (nDSC) is 1200 sub-carriers (DBW/sBW). Note that this is a particular deployment case, since LTE allows scalable BW and being the possibilities:

Spectrum Allocation	2.5 MHz	5 MHz	10 MHz	15 MHz	20 MHz
Subcarrier Spacing Δf	15 MHz				
Sampling Frequency f_s	3.84 MHz	7.68 MHz	15.68 MHz	23.04 MHz	30.72 MHz
FFT Size	256	512	1024	1536	2048
Number of Subcarrier	150	300	600	900	1200
RB per subframe	12	25	50	75	100

Table 3.1: Overview of LTE BW configurations

- *#Snapshots*: The number of snapshots depends on the simulated time and the desired time step. This will also has to take into account the minimum sampling frequency of the Doppler filter in order to avoid aliasing and represent it correctly. The number of snapshots defines the discrete time length of the Doppler filter, in order to know the total time length, it is necessary to divide it by the Doppler sampling frequency (f_{s_d}).
- *Channel model*: this pull-down list contains a set of channel models specified in the 3GPP and ITU-R recommendations. The recommendations specify different models, each one appropriate for a specific case (e.g. pedestrian, vehicular). For each of these cases, a multipath tap delay profile is specified as well as the number of multipath components.
- *Doppler sampling frequency*: As mentioned above, the total equivalent channel simulated time depends on the number of snapshots and the sampling frequency. So, if N is the total number of snapshots, the total time simulated (Time window) with the Doppler filter is $N \cdot T_{s_d}$ (where $T_{s_d} = 1/f_{s_d}$).

For the Doppler spread, two options can be chosen: to introduce directly the maximum Doppler frequency or to calculate it by using equation 2.1 and introducing the central frequency and the users' speed.

3.2.1 Reduction of the channel's values

Taking into account the reiteration and the desired randomness of the system, an important fact to take into account is that it can return improbable values. In order to reduce the amount of improbable represented values it is required to reduce the number of channel values. The main reason is to be able to quantify precisely the most probable values. If the deepest fadings are taken into account and the entire equidistant range is quantified, the most probable zones are going to be represented worse.

To assure this, only a 95% of the most probable values are going to be kept after generating the channel to do this, probabilistic tools are necessary.

3.2.1.1 95% values of the CDF

Common known probabilistic tools are the CDF (Cumulative Distribution Function) and the PDF (probabilistic density function). The CDF [16], or just distribution function, is a mathematical expression which describes the probability that a system will take on a specific value or set of values. More specifically, it describes the probability that a real-valued random variable X with a given probability distribution will be found at a value less than or equal to x . This is shown in equation 3.1, where for every real number x , the CDF of a real-valued random variable X is given.

$$x \rightarrow F(x) = P(X \leq x) \quad (3.1)$$

In order to keep a 95% of the values, the desired function is the CDF as it provides the accumulation, giving an idea of the most probable values in the margin.

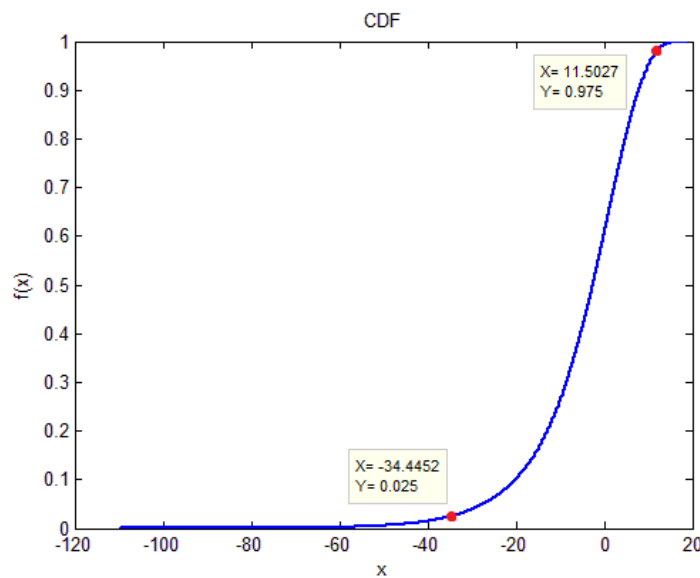


Figure 3.5: CDF example. nSnap=128, fd=5,5. ITU-ETU

Figure 3.5 shows an example of a CDF done with resulting values from a simulated channel. As mentioned above, if a 95% of the values are going to be taken it means the desired minimum value is given by the 2.5% and the maximum by the 97.5%. So, even if the range of values goes from -109.43 dB to 18,97 dB, the used margin will go from -34.44 dB to 11.5 dB as the rest of the values are given with less than a 2.5% of probability. This can be further understood by looking at the result shown in figure 3.8.

3.2.1.2 Alternative to the CDF procedure

The function used in the example from figure 3.5 is a mathematical function of MATLAB named `ecdf` which calculates the Kaplan-Meier estimate of the CDF, also known as the empirical cdf. As this function does not exist in C++ it has to be implemented. To simplify the programming and the computational resources used to perform this function, as an alternative, in the case of large size vectors, the cdf can be approximated by doing the following:

- 1) Transform the matrix into a vector of size $N = n\text{Snap} \cdot n\text{DSC}$.
- 2) Sort the values of the vector from the smallest to the greatest.

- 3) Choose the minimum as the value in the vector's position $[0.025 \cdot N]$
- 4) Choose the maximum as the value in the vector's position $[0.975 \cdot N]$

Using this approximation the result is as expected, if N is large enough the result is accurate. Following the example from figure 3.5, the maximum resulting value performing this algorithm is 11,5 dB and the minimum is -34,43 dB, a very good result if it is compared with the one from the CDF.

There are many sorting algorithms, some of the most popular ones are quicksort, bubble sort, heapsort and insertion sort among others. The most important factor in order to choose the most appropriate is the computational complexity given by the Big O notation. Bubble sort and insertion sort are discarded because they show worse performance ($O(n^2)$) as compared with quicksort and heapsort ($O(n \cdot \log(n))$). Heapsort is discarded due to its instability despite it is better in the worse time than quicksort e. Hence, given the advantages and drawbacks, the implemented sort algorithm has been the quicksort algorithm from [18]. The following table shows a comparison of some of the sort algorithms.

Sort	Time Average	Time Best	Time Worst	Space	Stability
Bubble sort	$O(n^2)$	$O(n^2)$	$O(n^2)$	Constant	Stable
Modified Bubble sort	$O(n^2)$	$O(n)$	$O(n^2)$	Constant	Stable
Selection Sort	$O(n^2)$	$O(n^2)$	$O(n^2)$	Constant	Stable
Insertion Sort	$O(n^2)$	$O(n)$	$O(n^2)$	Constant	Stable
Heap Sort	$O(n \cdot \log(n))$	$O(n \cdot \log(n))$	$O(n \cdot \log(n))$	Constant	Instable
Merge Sort	$O(n \cdot \log(n))$	$O(n \cdot \log(n))$	$O(n \cdot \log(n))$	Depends	Stable
Quicksort	$O(n \cdot \log(n))$	$O(n \cdot \log(n))$	$O(n^2)$	Constant	Stable

Table 3.2: Sort algorithm's comparison [17]

3.2.2 Quantification

As mentioned, the channel is going to be created and saved using the channel simulator, and then loaded at any time from the system simulator. The channel is a matrix of size $nSnap \cdot nDSC$, which is going to be saved in a binary file. Thus, the size of this file will be equal to $nSnap \cdot nDSC \cdot VarSize$, where $VarSize$ is the size of the type of data.

Due to the large dimensions of the matrix, it is important to minimize the data's type size. As the channel is a matrix of floating point numbers which occupy 4 Bytes (32 bits), the aim is to quantify it into an unsigned char in order to occupy the minimum space. Hence, this minimum space is one Byte (8 bits) which means it can achieve 256 values.

As an example, a channel is created with a Doppler sampling frequency of 1000 Hz and 16384 (2^{14}) snapshots, which equals 16,384 seconds of channel duration. If it is generated for 1200 subcarriers, the file size will change depending on the level of quantification as shown in table 3.3.

Data size	T_{Tot}	N_t	N_f	DIM
4 Bytes				150 MB
2Bytes	16,384 s	16384	1200	75 MB
1 Byte				18,75 MB

Table 3.3: Channel file size for various data sizes

By quantifying, the resolution worsens and an error is introduced. The resolution is defined by the steps between the closest values, so it is calculated as the range of values to quantify divided by the new number of possible new values, which is $(\text{Max}-\text{Min})/256$. Each value will be approximated by its closest in this range, so the maximum error introduced by quantification is equal to half the resolution. Following the same example used in the CDF section, the resolution results 0,179 dB so the maximum error is 0,089 dB, an acceptable error.

3.2.3 Final Results

The reduction of values and the quantification are done at the same time so the changes are significant.

On the one hand, as it can be appreciated by comparing figure 3.6 with 3.7 and figure 3.8 with 3.9, the represented signal in the figure on the right has sharper changes due to quantification. On the other hand, as the range has been reduced from 128,4 dB to 45,93 dB some maximum and some minimum values are cut, as it was expected due to the reduction of the values. Hence, notice that in the second couple of figures 0 equals -34,43 dB and 255 equals 11,5 dB.

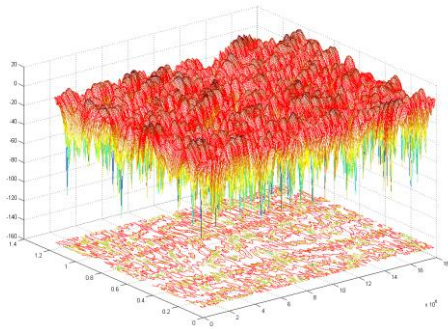


Figure 3.6: Channel representation before quantification

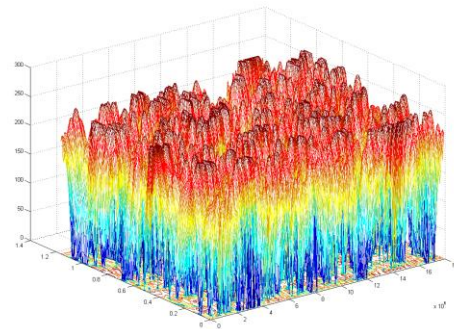


Figure 3.7: Channel representation after quantification

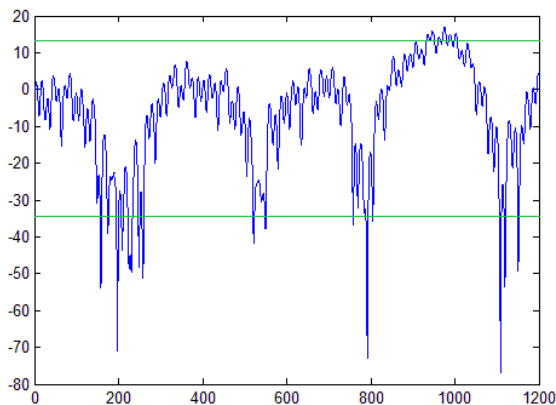


Figure 3.8: Channel representation before quantification and value reduction

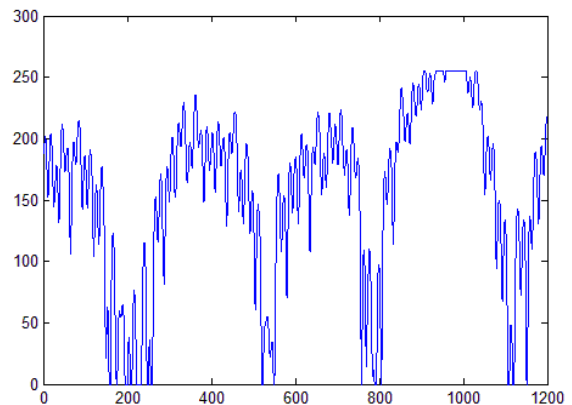


Figure 3.9: Channel representation after quantification and value reduction

3.2.4 Channel smooth

As explained in the first section of chapter 2, the final channel response is a combination of several contributions. First the path loss which corresponds to the propagation model, then the long term fading or shadowing model applied and finally, the short term fading or Fast fading. The short term fading is obtained by using the generated channel; in concrete, assigning a pointer to a position in the obtained matrix.

This assignation is done using a uniform variable of mean T_c and variance 1, so the users will see, in average, different channels. As the simulation time increases, the pointers will move along the matrix according to the user's mean speed. When a user gets to the end of the matrix, in the following time step it will start in the first position. So, in order to reduce the abrupt channel change, a smooth effect is done.

The smooth effect consists on adding positions to the matrix which will progressively weight the average between the values of the last row and the first one. The selected number of smooth rows has been four, so the weights have been done as follows, taking into account the alphabetical indexes shown in figure 3.10.

$$c=0.8 \cdot b+0.2 \cdot a \quad (3.1)$$

$$d=0.6 \cdot b+0.4 \cdot a \quad (3.2)$$

$$e=0.4 \cdot b+0.6 \cdot a \quad (3.3)$$

$$f=0.2 \cdot b+0.8 \cdot a \quad (3.4)$$

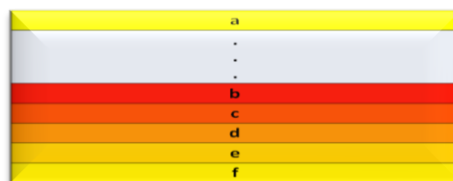


Figure: 3.10: Channel matrix smooth rows

CHAPTER 4. DEVELOPMENT OF A DYNAMIC LTE SIMULATION PLATFORM

As mentioned in the problem statement, one of the objectives of this project is to evaluate the system's performance under different degrees of feedback. This chapter presents the modifications and the new features developed over the existent static LTE system level simulator in order to achieve a dynamic LTE simulation platform. The results obtained from the implemented simulator are shown in chapter 5.

4.1 System simulator

The system's simulator main window is shown in figure 4.1. As it can be appreciated, the tabs contain a set of sections which contain the various simulation configurations. Some configurations pre-sets are: Layout and users, Simulation, OFDMA, Classes, PRB Management/Classes, Time structure/Classes, Pre-sets and RRM, Sites/Sectors (For more information see Annex A). Notice that the simulation configurations explained in the following sections are the ones which have a direct relationship with the work developed in this project.

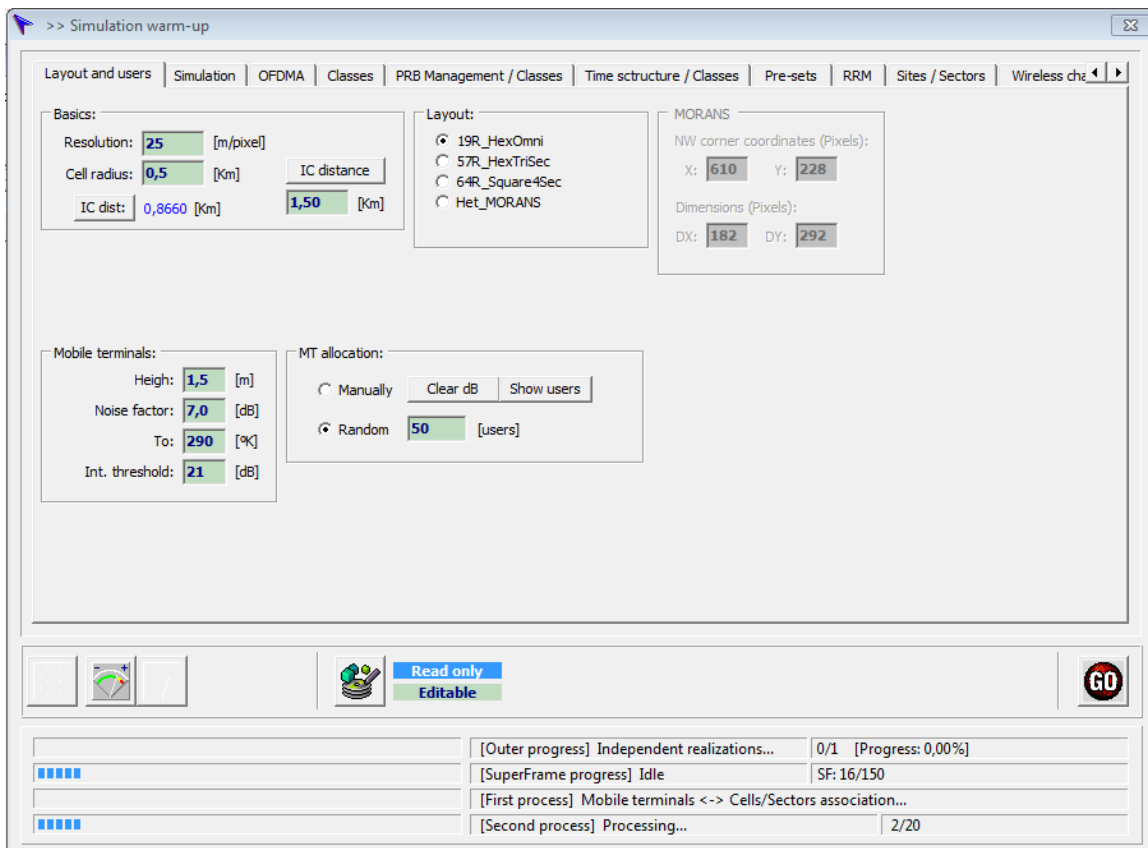


Figure 4.1 System simulator's warm-up window

4.1.1 User's movement and layout reduction

As mentioned previously, the users will move along the layout each time step, which has been decided to be one TTI (1 ms). This movement will be determined by a random direction for each user and a position displacement equivalent to the user's speed introduced when the channel was generated.

Statistically, a user does not change its direction with each time step. In this case a uniform random variable has been deployed, so it will change direction with a probability of 40%. Hence, if it changes direction it will not be drastically, for example 360° , as one user usually changes direction within a certain angle. The chosen angle, thought to be appropriate, has been 45° left and right from its original direction. This can be further understood by seeing figure 4.2.

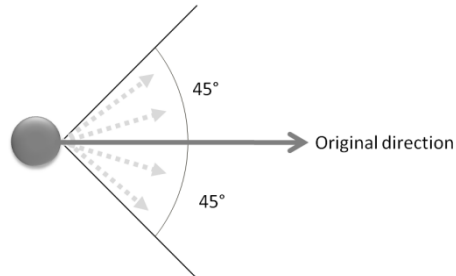


Figure 4.2: User's movement and direction change

The fact that the users move implies that they can exit the layout. To solve this, the simulator will have to decide which move is possible and which not. The first approach was to impose a user to bounce back in the same incidence angle when it got to the end of the simulation layout. The second approach was to reduce the evaluated zone of the layout to the centre cells. This approach was consequence of the fact that the users which are placed in the outer cells perceive less interference because they have less adjacent cells. For this reason statistics are also just collected from the central cell, which is the one that is correctly characterized from an interference viewpoint.

Statistically in a long period of time, it is shown that when a user enters a cell another user exits it. Under this assumption, the simulated zone will be only one cell, taking into account the interference from the rest of the cells. Moreover, it gives the advantage of reducing the simulation time as the number of users is reduced. So, as the users are placed in one cell, they will bounce if they reach the end of the cell. Two criteria have been implemented to limit their position. The first one consists on setting the threshold as the circle which is formed with the cell radius (figure 4.3a) and the second one consists on setting the threshold as the circle which is tangent to the cell border (figure 4.3b). The final implemented option has been the second one because in the first case users would be handovered from one cell to the other.

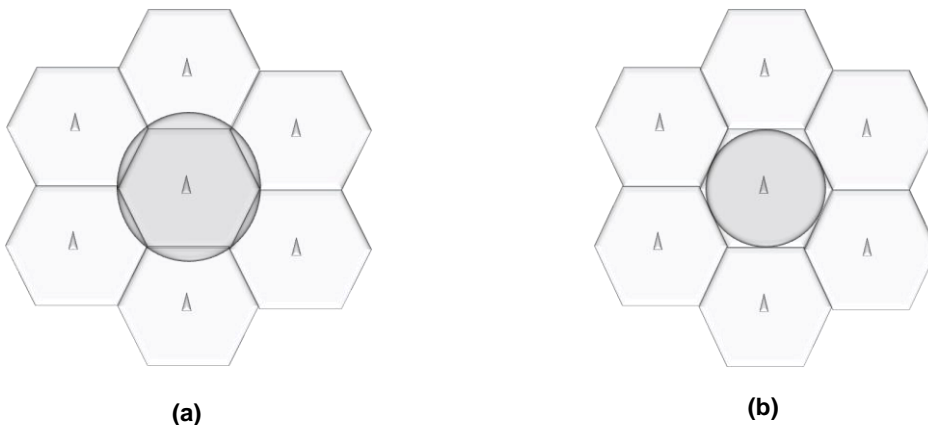


Figure 4.3: Implemented simulation threshold. **a)** Outer cell circular threshold, **b)** Inner cell circular threshold

4.1.2 Reference signals

The LTE standard defines three different types of Reference Signals (RSs), also known as pilot signals which are constantly transmitted in the DL. The reference signals are used for cell search and initial acquisition, DL channel estimation for coherent demodulation/detection at the UE, and DL channel quality measurements. This section explains the LTE RS design in order to understand how it has been implemented in the simulator, explained in section 3.3.3.2. It is not unusual missing the RS in system level simulations and just considering that the whole band can be monitored without restrictions.

4.1.2.1 Reference signals in LTE

As mentioned above, three different types of RS are provided in the LTE DL [19]:

- Cell-specific RSs (often referred to as common RSs, as they are available to all UEs in a cell)
- UE-specific RSs, which may be embedded in the data for specific UEs
- MBSFN-specific RSs, which are only used for Multimedia Broadcast Single Frequency Network (MBSFN) operation

The most important RSs are the Cell-specific, the others are additional RS, and so the in the following just the Cell-specific RSs are detailed.

In general, the complex values of the reference symbols will vary between different reference-symbol positions and also between different cells [24]. Thus, the reference signal of a cell can be seen as a two-dimensional sequence, in the LTE specifications referred to as a two-dimensional reference-signal sequence.

The LTE system has been conceived to work under really high-mobility assumptions, in contrast to previous cellular systems and even more with respect to WLAN systems which are generally optimized for pedestrian-level mobility.

The required spacing in time between the reference symbols can be obtained by considering the maximum Doppler spread (highest speed) to be supported, which for LTE corresponds to 500 km/h. The Doppler shift is $f_d = (f_c \cdot v/c)$ where f_c is the carrier frequency, v is the UE speed in metres per second, and c is the speed of light ($3 \cdot 10^8$ m/s). Considering $f_c = 2$ GHz and $v = 500$ km/h, then the Doppler shift is $f_d \approx 950$ Hz. According to Nyquist's sampling theorem, the minimum sampling frequency needed in order to reconstruct the channel is therefore given by $T_c = 1/(2 f_d) \approx 0.5$ ms under the above assumptions. This implies that two reference symbols per slot are needed in the time domain in order to estimate the channel correctly.

In the frequency domain there is one reference symbol every six subcarriers on each OFDM symbol which includes a reference symbol, but these are staggered so that within each RB there is one reference symbol every 3 subcarriers, as shown in figure 4.4. This spacing is related to the expected coherence BW of the channel, which is in turn is related to the channel D_s . In particular the 90% and 50% coherence bandwidths are given respectively by $B_{c,90\%} = 1/50\sigma_T$ and $B_{c,50\%} = 1/5\sigma_T$ where σ_T is the r.m.s delay spread. In [25] the maximum r.m.s channel D_s considered is 991 ns, corresponding to $B_{c,90\%} = 20$ kHz and $B_{c,50\%} = 200$ kHz. In LTE the spacing between two reference symbols in frequency, in one RB, is 45 kHz, thus allowing the expected frequency domain variations of the channel to be resolved.

The RS sequence also carries unambiguously one of the 504 different cell identities, N_{ID}^{Cell} . For the cell-specific RSs, a cell-specific frequency shift is also applied, given by $N_{ID}^{Cell} \bmod 6$. This shift can avoid time-frequency collisions between common RS from up to six adjacent cells. Avoidance of collisions is particularly important in cases when the transmission power of the RS is boosted, as it is possible in LTE up to a maximum of 6 dB relative to the surrounding data symbols. RS power boosting is designed to improve channel estimation in the cell, but if adjacent cells transmit high-power RS on the same Resource Elements (REs) the resulting inter-cell interference would be prohibitive. It is important to notice, though, that in LTE the eNodeBs do not transmit in a synchronized manner, so if in a particular moment one eNodeB is transmitting a RS, it is improbable that the other BS are transmitting RS as well, so the data symbols from other BS could be interfered by the RSs.

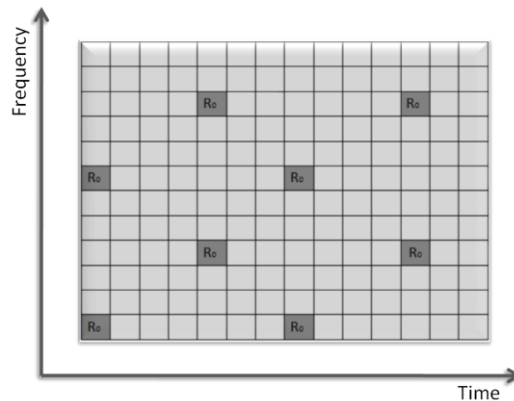


Figure 4.4: Cell-specific reference symbol arrangement in the case of normal CP length for one antenna port.

4.1.2.1.1 UE-specific RSs

UE-specific RS may be transmitted in addition to the cell-specific RSs. They are embedded only in the RBs to which the PDSCH is mapped for UEs which are specifically configured (by higher-layer RRC signalling) to receive their DL data transmissions in this mode.

The MBSFN-specific RSs will not be explained here as it is not part of this research.

4.1.2.2 Implemented RSs

The implemented cell-specific RSs have been designed only in the frequency domain, while in time it remains constant because of the timing consideration of this project.

While the minimum time studied is one TTI, in LTE the minimum time consideration is one OFDM symbol, in concrete, one slot is comprised by seven OFDM symbols. Figure 4.4 shows that the granularity of the RS's is of one OFDM symbol. So, at the measurement instant, once every TTI, the reference signals will be measured every 3 RBs, instead of 6 in the case of each OFDM symbol transmitting RSs, as shown in figure 4.5.

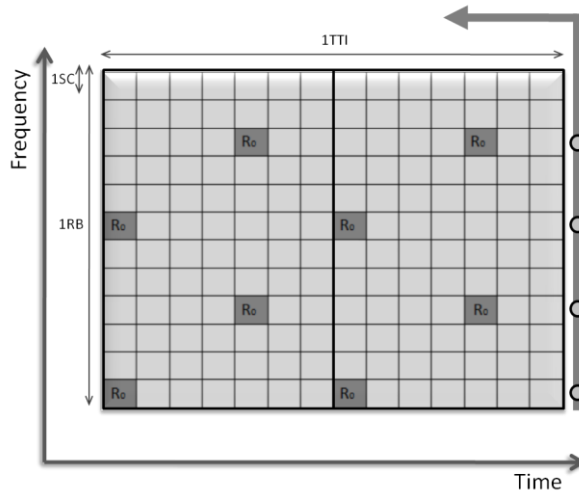


Figure 4.5: RSs observed every TTI

In order to vary the positions of the reference signals in each cell, a cell-specific frequency shift equal to one has been applied in the system simulator for each adjacent cell. The cell patron is repeated every three sites due to the frequency separation between the measured RSs is of three SCs, so if the mentioned shift is of one, the separation between cells which place a reference signal in the same subcarriers is three. This can be further understood by looking at figure 4.6.

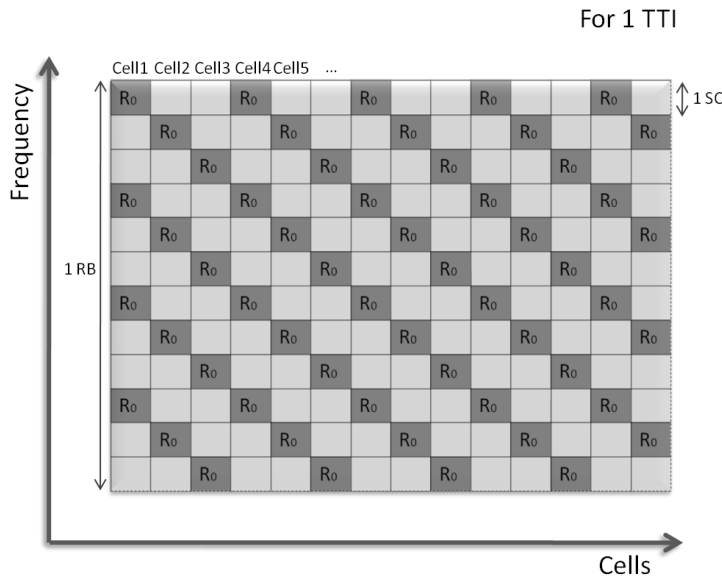


Figure 4.6: Implemented Cell-specific RSs for one TTI

In the original simulator, there were no reference signals distinctions so the power assigned to each SC was equally distributed as the mean value:

$$\overline{P_{SC}} = \frac{P_{TXeNodeB}}{N_{RB} \cdot N_{SC}} \tag{3.5}$$

Where,

- $P_{TXeNodeB}$ is the total available power at eNodeB
- N_{RB} is the number of RBs per eNodeB
- N_{SC} is the number of SC per RB

So, for example, if an eNodeB can transmit 43dBm among 100 RB and each RB has 12 SC, each SC will be assigned 12.02 dBm (12.21 mW).

The power of the reference signal is not defined in the standard, so it has been decided to be a 10% higher than the mean SC power. The rest of the power will be equally distributed among the remaining SCs (equations 3.6 and 3.7).

$$P_{RS} = \overline{P_{SC}} \cdot 1.1 \quad (3.6)$$

$$P_{SC}' = \frac{P_{TXeNodeB} - P_{RS} \cdot N_{RS} \cdot N_{RB}}{N_{SC}'} \quad (3.7)$$

Where,

- P_{RS} is the RS power
- N_{RS} is the number of RSs
- P_{SC}' is the power of a data SC
- N_{SC}' is the number of a data SC

4.1.3 CQI Feedback compression schemes

The main new feature in the channel feedback, explained in section 2.2.2, is the frequency selectivity of the report. The periodicity and frequency resolution to be used by a UE to report CQI are both controlled by the eNodeB. In the time domain, both periodic and aperiodic CQI reporting are supported [19].

Since providing a full 4 bit CQI for all the PRBs would mean excessive uplink signalling overhead of hundreds of bits per sub-frame, some feedback compression schemes are used. To reduce feedback, the CQI is reported per sub-band basis. The size of the sub-bands varies depending on the reporting mode and system BW from two consecutive PRBs up to whole system BW. The feedback compression scheme developed in this project has been based in the compression methods explained in [13] and [19].

4.1.3.1 Aperiodic CQI Reporting

The aperiodic CQI reporting methods are the following:

- **Ideal feedback.** This reporting method is used in this project to define the feedback where a CQI value is reported for each RB in the whole system BW. An example is represented in figure 4.7.

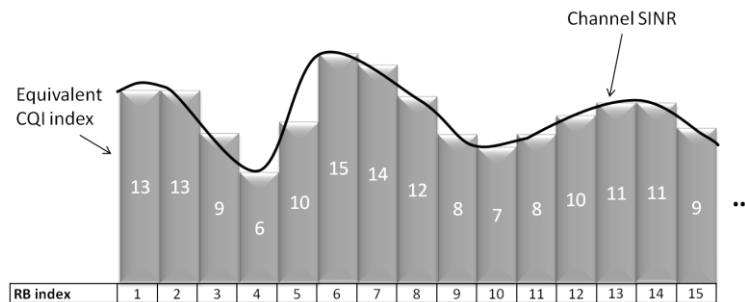


Figure 4.7: Example for ideal CQI reporting

- **Wideband feedback.** The UE reports one wideband CQI value for the whole system BW. The same example as before, but wide the wideband method is shown in the following figure.

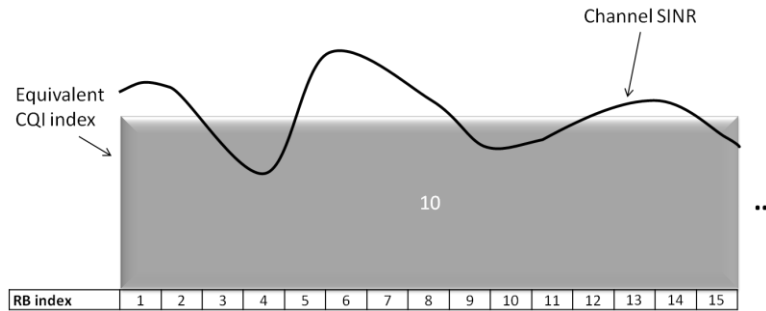


Figure 4.8: Example for wideband CQI reporting

- **eNodeB-configured sub-band feedback.** The UE reports a wideband feedback. In addition, the UE reports a CQI value for each sub-band, calculated assuming transmission only in the relevant sub-band. An example for this feedback is shown in figure 4.9. Sub-band CQI reports are encoded differentially with respect to the wideband CQI using 2-bits as follows:

$$\text{Sub-band differential CQI offset} = \text{CQI index}_{\text{Sub-band}} - \text{CQI index}_{\text{Wideband}}$$

The possible sub-band differential CQI offsets are $\{\leq -1, 0, +1, \geq +2\}$. The sub-band size k is a function of system BW as summarized in table 4.1.

System BW (RBs)	Sub-band size (k RBs)
6-7	(Wideband CQI only)
8-10	4
11-26	4
27-63	6
64-110	8

Table 4.1: Sub-band size k versus system BW

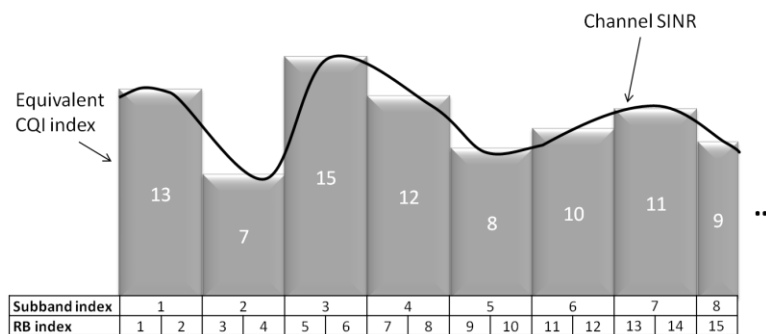


Figure 4.9: Example for eNodeB-configured sub-band CQI reporting

- **UE-selected sub-band feedback (also named Best-M average).** This method is an effective compromise between the system performance and the uplink

feedback signalling overhead. In Best-M average reporting the UE first estimates the channel quality for each sub-band. Then it selects the M best ones and reports back to the eNodeB a single average CQI corresponding to the MCS/TBS the UE could receive correctly assuming that the eNodeB schedules the UE on those M sub-bands. The parameter M depends on the system BW and corresponds to roughly 20% of the whole system BW. Table 4.2 gives the k and M values given for each system BW range while figure 4.10 shows the principle of the Best-M average compression scheme.

The CQI value for the M selected sub-bands for each codeword is encoded differentially using 2-bits relative to its respective wideband CQI as defined by:

$$\text{Differential CQI} = \text{Index}_{\text{average } M \text{ preferred sub-bands}} - \text{CQIindex}_{\text{Wideband}}$$

The possible differential CQI values are $\{\leq +1, +2, +3, \geq +4\}$.

System BW (RBs)	Sub-band size (k RBs)	Number of preferred sub-band (M)
6-7	(Wideband CQI only)	(Wideband CQI only)
8-10	2	1
11-26	2	3
27-63	3	5
64-110	4	6

Table 4.2: Sub-band size k versus system BW

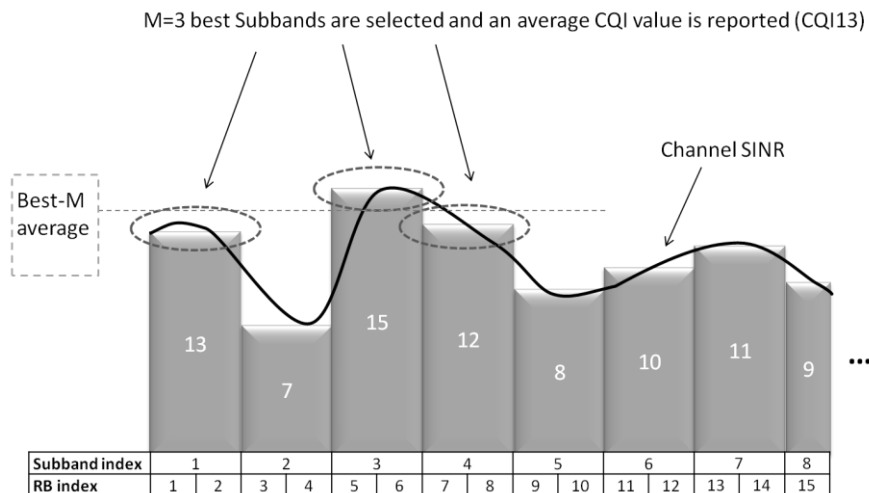


Figure 4.10: Example for the Best-M average. An average CQI value is reported for the M best sub-bands

These three reporting methods have been implemented in the simulator, but only periodic reporting has been simulated. So, the studied CQI reporting are the ideal, the wideband and the UE-selected sub-band feedback. Notice that the ideal feedback is the one which reports the CQIs which would correspond to each RB of the whole BW.

4.1.3.2 Periodic CQI Reporting

As mentioned above only wideband and UE-selected sub-band feedback are possible for periodic CQI reporting, for all DL transmission modes.

Note that in the UE selected sub-band case, the total number of sub-bands N is divided into J fractions called BW parts. The value of J depends on the system BW as summarized in table 4.3. In case of periodic UE-selected sub-band CQI reporting, one CQI value is computed and reported for a single selected sub-band from each BW part, along with the corresponding sub-band index.

System BW (RBs)	Sub-band size (k RBs)	Number of BW parts (J)
6-7	(Wideband CQI only)	1
8-10	4	1
11-26	4	2
27-63	6	3
64-110	8	4

Table 4.3: Sub-band size (k) and BW parts (J) versus DL system BW

4.1.4 Hybrid ARQ

As explained in [25] the usual approach to handle transmissions errors is to use Automatic Repeat Request (ARQ). In an ARQ scheme the receiver uses an error-detecting code, typically a Cyclic Redundancy Check (CRC), to detect if the received packet is in error or not. If no error is detected in the received data packet, the received data is declared error-free and the transmitter is notified by sending a positive acknowledgment (ACK). On the other hand, if an error is detected, the receiver discards the received data and notifies the transmitter via a return channel by sending a negative acknowledgment (NAK). In response to a NAK, the transmitter retransmits the same information.

Virtually all modern communication systems employ a combination of forward error-correcting coding and ARQ, a combination known as hybrid ARQ (HARQ). HARQ uses forward error correcting codes to correct a subset of all errors and rely on error detection to detect incorrigible errors. Erroneously received packets are discarded and the receiver requests retransmissions of corrupted packets. The HARQ controller provides the set of UE's that have to undergo a retransmission. In this case it is synchronous and adaptative, which means that retransmission can take place anywhere in the BW but in a specific TTI.

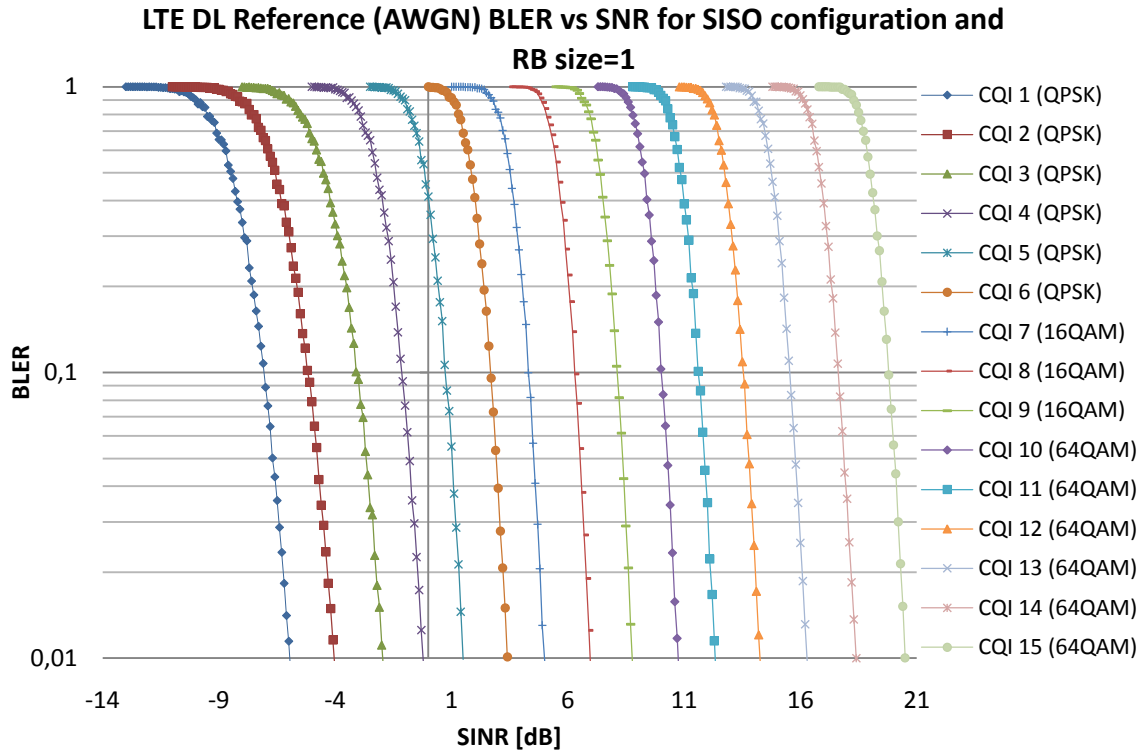
In a physical layer HARQ operation the receiver also stores the packets with failed CRC checks and combines the received packet when a retransmission is received. The HARQ operation in LTE supports both soft combining and the use of incremental redundancy [13]. The use of soft combining means that retransmission has exactly the same rate matching parameters as the original transmission and thus exactly the same symbols are transmitted. For incremental redundancy, the retransmission may have different rate matching parameters like the original transmission.

4.1.4.1 HARQ implementation

As explained in section 2.2.2, the UE reports back to the eNodeB the CQI index such that under the current radio conditions the estimated received DL transport block BLER shall not exceed 10%. As mentioned above, the UE reports the detected errors by sending NAKs.

The amount of errors of each UE is determined in the simulation by using a uniform random variable. This random variable will be compared with the equivalent instantaneous BLER (according to the channel state) in order to determine whether the

user has been able to recover the transport block correctly. The equivalent instantaneous BLER is the one which corresponds to the instantaneous SINR of the user, in the entire band, and its assigned MCS. The MCS will be handled as the CQI value they are considered to be dual, although in practice there are more MCS options than CQI values, but for the sake of simplicity (and without losing generality) duality has been considered. Figure 4.11 shows the relation between BLER and SINR (Signal to Interference plus Noise Ratio) for each CQI value.



It takes a certain amount of time for the HARQ ACK/NAK to be received and for the system to be ready to retransmit if needed. The time interval between two successive HARQ transmissions is typically 8 ms in LTE, an entire Round-Trip Time (RTT) [26]. During these 8 ms, the transport block can either be transmitted (if received with errors) or be discarded from the transmitting buffer (if received without errors), as it is shown in figure 2.6 from section 2.2.2.

In order to take into account this, the simulator will check each evaluation time if the information sent 8ms before is. In the case it did, and the user is retransmitting, the instantaneous SINR will be multiplied by two as the equivalent BLER requires half the SINR.

On each transmission, at the receiving end, the information is kept despite it is not received correctly. On the following transmission the eNodeB, will send a different part of the transport block, so at the receiving point, this information is combined with the one sent previously in order to check if it is now able to recover the sent data. At this point, as the receiver has more information than previously, the required SINR is less in order to obtain the same value of BLER or similarly, with the same level of SINR the BLER would be less. In LTE a maximum of 4 HARQ retransmissions are allowed, otherwise the packet is discarded. In the case of this simulator, only one retransmission

is considered in order to evaluate how many transmissions are discarded in these conditions.

The procedure followed in this project to perform the HARQ is pictured in the following diagram. Note that a new retransmission increases the energy of the useful signal in 3 dB and that is why the SINR is multiplied by 2 in linear units:

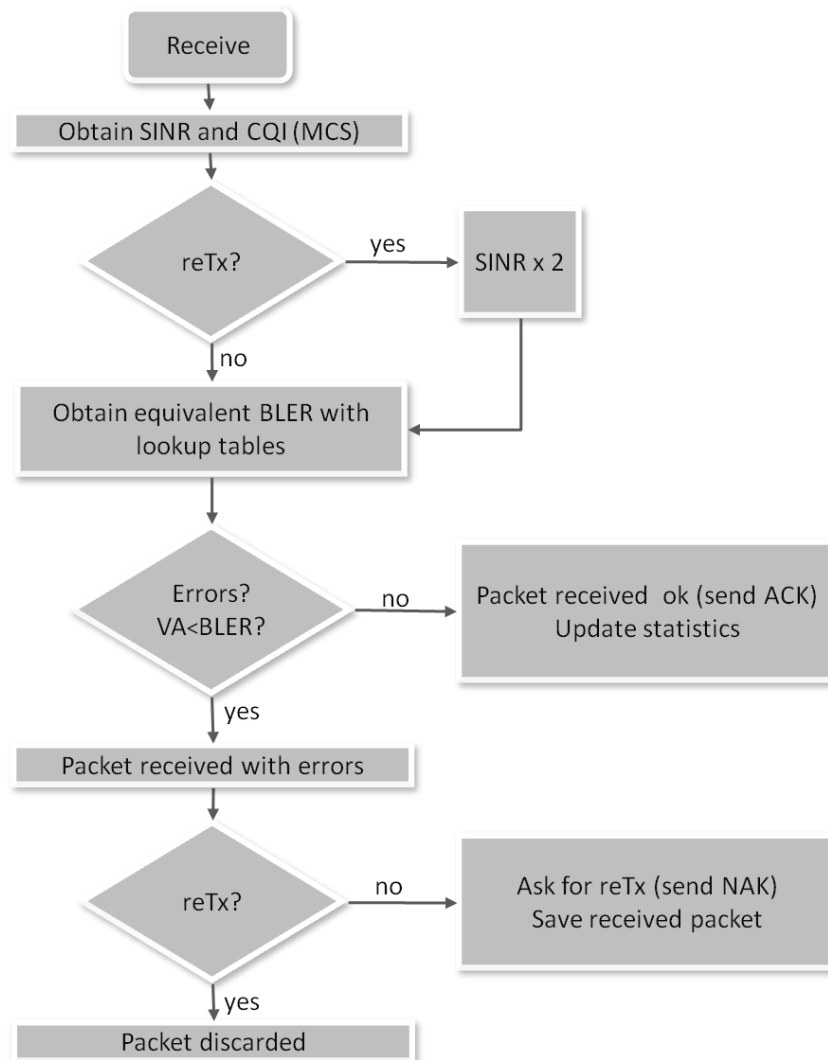


Figure 4.12: Implemented HARQ flow chart for each user and TTI

CHAPTER 5. SIMULATIONS

Once the channel simulator and the modifications of the system simulation have been explained, the next step is to obtain results in order to compare the different strategies. As the modifications introduced to the system simulator gives more realism to the simulations, the resulting performance of the system DL should be worse than the ones obtained with the original simulator which ran under ideal characteristics. The results obtained with the original static simulator are shown in Annex A.

5.1 Fast fading channel parameters

As mentioned previously, the channels used for the evaluations, are generated in the channel simulator and then loaded in the system simulator. In order to reduce the size of the channel matrix and in this way reduce the memory used in the program, three different channels will be generated for each model as well as a pointer associated to each user in order to place them among these three matrixes. Thus, the pointer will be generated taking into account each user has to experience a different fast fading channel, so they will be placed along the matrixes using a uniform random variable with the mean value equal to T_c . Remember T_c is the expected time duration over which the channel's response to a sinusoid is essentially invariant. Table 4.1 shows various values of T_c associated to each speed taking into account the centre frequency is 2.14 GHz.

Speed (Km/h)	fd (Hz)	Tc (ms)
3	5,944	30,112
6	11,889	15,056
10	19,815	9,034
25	49,537	3,613
50	99,074	1,807
75	148,611	1,204
100	198,148	0,903
120	237,778	0,753

Table 5.1: Tc and Ts_dopler for diferent values of UE's speed. Fc=2,14GHz

With each time step of the simulation, the pointer will move according to the user's mean speed, which is the one determined when the channel was generated. So, when the users move they will move along the matrix experiencing the time evolution of the fast fading channel. The shadowing and the path loss also change with the user's movement.

The fast fading channel depends on the Doppler's filter parameters to model the time domain characteristics and the ITU (International Telecommunication Union) channel models to model the frequency domain. The parameters of these combinations are shown in the following table.

Speed (Km/h)	fd (Hz)	ITU Model	Number of snapshots	sBW (KHz)	DBW (MHz)	Doppler's fs (Hz)
3	5,944	Extended vehicular A [32,5 ns grid]	1024	15	18	1000
25	11,889	Extended vehicular A [32,55 ns grid]	1024	15	18	1000
120	19,815	Extended vehicular A [32,55 ns grid]	1024	15	18	5000

Table 5.2: Channel's simulation parameters

5.2 Simulation parameters

This section shows the main parameters of the simulation regarding the new modifications. The rest of the parameters are shown in detail in section A.3 of ANNEX A.

The simulation is done over a multicell scenario, a central one which is surrounded by two rings (LTE defined Macro 1 case scenario). The processes are executed and statistics are collected just in the central cell, it is considered that all the other cells on the scenario are transmitting. Finally, the number of users spread in this central cell is always 20.

The scheduler used is Proportional Fair (PF) which is a compromise-based scheduling algorithm. It is based upon maintaining a balance between two competing interests: Trying to maximize total wireless network throughput while at the same time allowing all users at least a minimal level of service. This is done by assigning each data flow a data rate or a scheduling priority that is inversely proportional to its anticipated resource consumption [32]. To assure the PF works correctly it has to be simulated during a sufficient time period. The value decided to be appropriate, which is a compromise with the simulation time, is of 300 TTI which equals 300 ms.

5.3 Performance evaluation

The following sections show the results obtained by running 20 users during 150ms varying the periodic feedback compression scheme and the UEs speed.

The represented results taken from the simulator in order to compare the different strategies are:

- CDF of the UEs throughput
- Percentage of assigned CQI values (shown in section 2 of Annex A)
- Percentage of assigned CQIs and received correctly by the UEs (shown in section 2 of Annex A)

Apart from studying the UEs throughput and the assigned CQI indexes, it is also interesting to observe other factors as the ones listed below:

- UEs without coverage
- Percentage of assigned UEs which received correctly the data
- Percentage of times there were retransmissions (1st reTx)
- Percentage of times the packets were discarded after the first retransmission failed

- Mean instantaneous BLER value

5.3.1 Ideal CQI feedback

This feedback reporting is named ideal because the UE reports a value for every RB in the whole band. By using this reporting scheme the eNodeB can allocate the resources in a fairer manner as it will have concern of each good part of the band for every user. If the conditions of the UE do not change significantly from one TTI to another, they will always obtain some part of the band. Thus, the eNodeB will assign the RBs to the UEs in those areas with the best conditions, so a large amount of users will transmit in each time step but in a small amount of RBs. This behaviour is pictured in figure 5.1, as the UEs' speed increases the UEs' throughput rates decreases.

Looking at table 5.3 it can be appreciated that the reduction of throughput is due to at higher speed, the errors increase leading to a further data loss. This loss of accuracy is because as the UE moves faster the channel changes in a faster way too, implying that at the evaluation instant the channel could have changed and the reception fails.

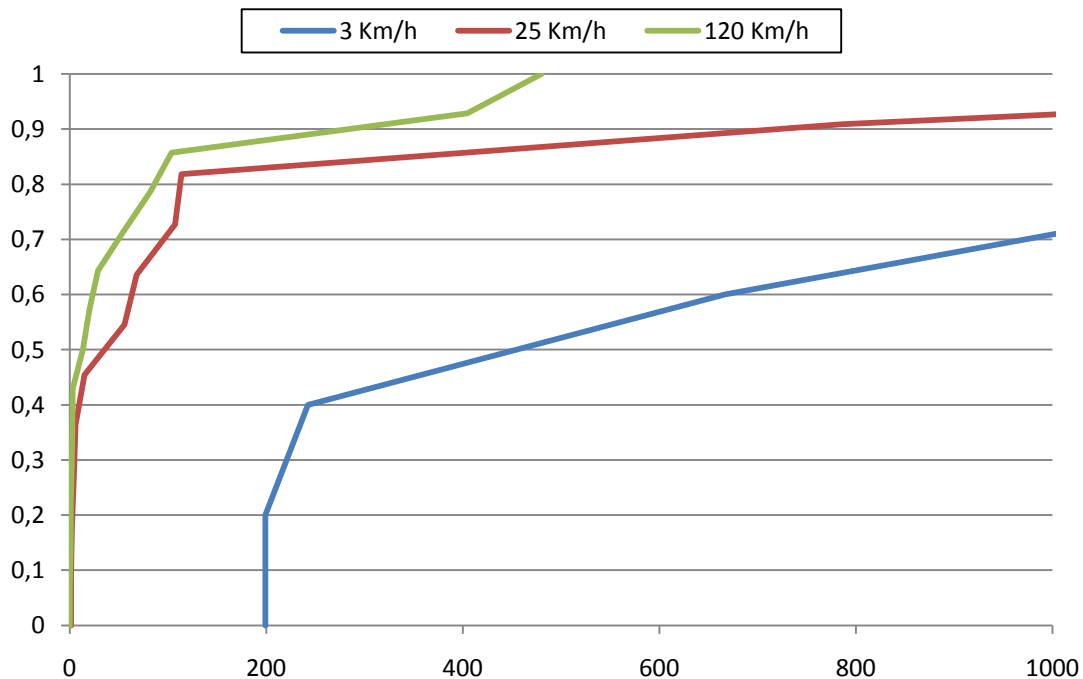


Figure 5.1: Ideal feedback. UEs' throughput CDF

UEs' speed	UEs' without coverage (%)	Received correctly (%)	reTx but not discarded (%)	Discarded	Mean BLER	Total with errors
3km/h (ExtVehicA)	4,07	93,88	6,12	0	9,13	6,12
25km/h (ExtVehicA)	2,9	63,27	36,05	2,04	36,15	38,09
120km/h (ExtVehicA)	3,27	27,89	67,35	7,48	72,28	74,83

Table 5.3: Ideal feedback. Simulation results

As shown in table 5.3, the mean BLER corresponds to the 10% BLER objective initially established in the link adaptation unit. As the speed increases, the channel changes faster so due to the outdate, the initially set BLER value is not accomplished. An option to reduce the retransmissions would be to fix a lower BLER objective based on the users' speed. It could be possible to estimate the speed in a fine manner from the Doppler deviation, and in a coarser manner through the number of reselections per minute in case the user is in an idle mode or through the handovers per minute when it is active.

5.3.2 Wideband CQI feedback

The wideband CQI feedback is the one which gives less information of the user's state along the frequency BW. As the UE only reports one CQI value for the whole band, if a UE reports a high CQI value, the eNodeB will believe the UE has in average good channel conditions so it will assign a larger amount of RB compared to the ideal reporting. On the other hand, it will be more restrictive assigning resources to UEs with bad conditions leading to a larger difference in throughput between UEs with good and bad conditions.

The UEs' throughput CDF obtained using this CQI feedback is shown in figure 5.2. Observing the results in table 5.5, it can be concluded that under these conditions there are more errors than using the ideal feedback method. This is understandable because the user only gives one identifier regarding the whole band, and the scheduler may allocate a RB in which actually there are no good transmitting conditions. This is reflected on the results of table 5.4 at low speeds there is a loss of throughput.

Users' speed	Throughput achieved by 50% of users Ideal	Throughput achieved by 50% of users Wideband
3 Km/h	450 kbps	20kbps
120 Km/h	13 kbps	25 kbps

Table 5.4: Throughput achieved by 50% of users. Ideal and Wideband feedback for 3 and 120 Km/h

In the case of high speeds, the results obtained of mean throughput are lower in the ideal feedback case. A possible explanation for this behaviour could be that when the user moves at a low speed, the scheduler would allocate resources without knowing the exact behaviour of the channel, so there are going to be a considerable amount of retransmissions. As the channel changes slowly, many packets are being discarded. What it is important to highlight is that as the user moves faster the channel conditions will change more dynamically, so all these retransmissions occurred due to the fact that the scheduler does not have much concern of the channel conditions, have more chance of being received correctly and so the maximum throughput increases. This behaviour is close to the one having a random assignation value of CQI; although it is a good criterion useful to order users, it is not a useful method to choose which resources are better for the users, as more errors would be committed in this assignation, it is probable that in some of this resources may be in a fading.

So, even though there are more retransmissions, if a UE is under a deep fading and the UEs move at a low speed, the channel will hardly change when the retransmission is received, while, if the UEs move faster it is more likely that it leaves the deep fading leading to a correct reception of the information.

It would be interesting, as a future work, to investigate the opposite impact of the throughput in relation to the ideal case.

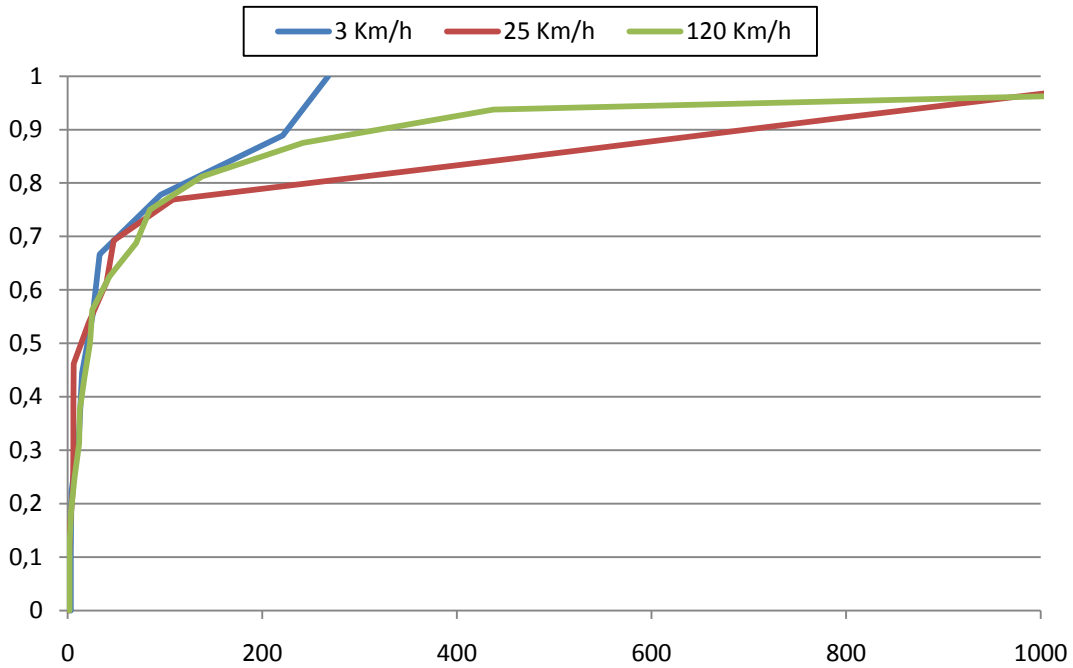


Figure 5.2: Wideband feedback. UEs' throughput CDF

UEs' speed	UEs' without coverage (%)	Received correctly (%)	reTx but not discarded (%)	Discarded	Mean BLER	Total with errors
3km/h (ExtVehicA)	4,07	40,82	59,18	0	59,87	59,18
25km/h (ExtVehicA)	2,9	30,43	63,77	9,42	70,18	73,19
120km/h (ExtVehicA)	3,27	37,68	57,97	5,8	62,19	63,77

Table 5.5: Wideband feedback. Simulation results

Following the same idea, comparing table 5.5 with table 5.3, the BLER value for high speed is lower than in the ideal case. On the other hand, at low speeds the BLER worsens with the wideband method.

Summarising, at the highest speed the wideband method performs better because, despite more errors occur, the scheduler will allocate many resources with good CQI indexes, which at the moment may not be correct because of the average CQI reporting, but, when evaluating (8ms later) the channel may have changed and the throughput received is large. If a retransmission is required then the channel change plus the diversity applied by the HARQ increase the probability of receiving correctly. The performance of the ideal method at higher speeds is lower than the wideband is because the scheduler is allocating there where the UE has better transmission conditions, giving place to a small amount of errors. Also the MCS assigned tend to be lower in the ideal case.

5.3.3 UE-selected sub-band feedback

This reporting scheme is an intermediate case between the ideal method and the wideband method. As explained in chapter 3, the sub-band size (k) and the number of

preferred sub-band (M) are configurable. As the system BW in the simulations is configured to a 100 RBs, the corresponding configuration is $k=4$ and $M=6$. Other configurations have been deployed in order to study the results. If the value k is increased, the reporting is less accurate and it behaves similar to the wideband feedback. And as these values decrease, it behaves more as the ideal, which is $k=1$. The following figure shows the results for $k=6$ and $M=4$.

Note that the results in this case are closer to the ones obtained with the wideband method, because only two different values are finally reported. In this case the eNodeB will not allocate the resources in a fair manner as it is done with the ideal case, but it will not be so restrictive due to the scheduler has some extra information.

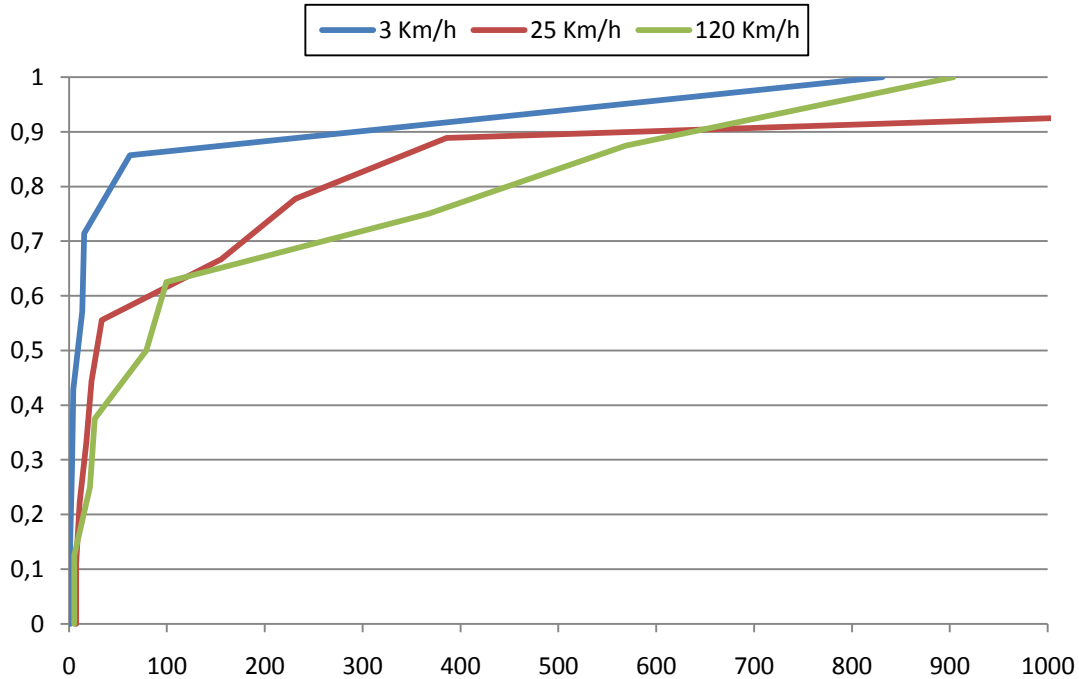


Figure 5.3: Best M feedback, $k=6$ and $M=4$. UEs' throughput CDF

UEs' speed	UEs' without coverage (%)	Received correctly (%)	reTx but not discarded (%)	Discarded	Mean BLER	Total with errors
3km/h (ExtVehicA)	4,07	50	50	2,08	51,49	52,08
25km/h (ExtVehicA)	2,9	44,12	54,41	2,94	55,47	57,35
120km/h (ExtVehicA)	3,27	29,29	68,57	5	70,11	73,57

Table 5.6: Best M feedback, $k=6$ and $M=4$. Simulation results

Comparing table 5.6 with 5.5 and 5.3, the numerical values reflect what it is above said. The best-M method performs closer to the ideal one at high speed having 2.17% of BLER difference, while the difference with the wideband is of 7.92%. At low speeds its behaviour gets closer to the wideband method having a difference of 8.38% in BLER, while in this case the difference rises up to 42.36% in the ideal case. This reflects how

sensitive the system is to the lack of information in terms of channel knowledge at lower speed, but as mentioned above, this fact is less relevant at high speed.

CONCLUSIONS

Along this project a dynamic and realistic LTE system simulator has been developed. The main tools for this purpose have been: Borland as the C++ compiler and MATLAB as the tool to represent the results of the simulator.

Regarding the simulator, all the proposed dynamic changes have been applied satisfactory in the original software platform at the Wicomtec research group. These were grouped in two differentiated stages of work.

Stage 1: Dynamic short-term fading channel. Different approaches from the specialized literature were revised and compared, the final selected option is Young's and Bealieu's IDFT model because the other option presented problems with aliasing. In order to reduce the required memory a smart pointer based system has been devised and the channel has been quantized considering the 90% percentile of its likely values.

Stage 2: After the integration of the channel model into the system level simulator, several changes were made on this one:

- The users' mobility and layout reduction
- Incorporation of RSs in order to be able to measure the channel quality
- HARQ scheme, providing the simulator with a retransmission module which makes it even closer to reality
- Various CQI reporting methods in order to simulate and evaluate its performance in a comparative manner.

As it was expected, the application of realistic features introduces factors which decrease the users' conditions, resulting in a degradation of the performance compared to the static LTE simulator which works over ideal theoretical conditions.

With the programmed dynamic LTE simulator, various CQI feedback reporting have been simulated, evaluating its performance. Under the simulation conditions it has been observed that at lower speeds, the ideal feedback is the best option with the drawback of introducing a high charge of signalling to the network, besides, this transmission is done by a power limited device, the UE. At high speeds, the randomness of the wideband option seems to partially compensate the number of errors and thus performs better, with the advantage of transmitting less reporting information leading to be a good option to be considered in these conditions. In order to obtain a compromise between both methods, the solution is to use the Best M feedback method. The work should be continued to further study the speed impact in non ideal cases and analyse its opposite impact when compared with the ideal case.

This project opens several lines for further long-term investigation as for example developing different types of traffic models, being capable of distinguishing data from voice users, and making the system capable of assuring the desired SINR target in order to be able to run that service. There are also some changes to do regarding the scenario, such as applying trisectorial antennas to the cells; to improve the scenario's performance, different schedulers and ICIC techniques could be applied in order to make fairer the distribution of RB's among users and also to reduce the interference impact, respectively. Another interesting future work could be to investigate different methods for users to report up to date channel quality to the eNodeB while maintaining the charge of signalling in a reasonable level.

ACRONYMS

ACK: Positive Acknowledgment

AMC: Adaptive Modulation and Coding

AR: Auto-regressive

ARQ: Automatic Repeat Request

AWGN: Adding White Gaussian Noise

BLER: Block Error Rate

B_s : Signal's BW

B_c : Coherence BW

BW: Bandwidth

CDF: Cumulative Distribution Function

CP: Cyclic Prefix

CSI: Channel State Information

CRC: Cyclic Redundancy Check

CQI: Channel Quality Indicator

DFT: Discrete Fourier Transform

DTFT: Discrete-Time Fourier Transform

D: Mean delay

DBW: Total channel BW

DL: Downlink

D_s : Delay Spread

eNodeB: Evolved Node B

EPC: Packet Core Network

f_c : Centre frequency

f_d : Maximum Doppler frequency

FDMA: Frequency Division Multiple Access

FDD: Frequency-Division Duplex

FFT: Fast Fourier Transform

FGN: Filtered Gaussian Noise

FIR: Finite Impulse Response

f_m : Maximum Doppler frequency normalized by the sampling rate

HARQ: Hybrid ARQ

HSPA: High Speed Packet Access

IDFT: Inverse Discrete Fourier Transform

IFFT: Inverse Fast Fourier Transform

i.i.d.: Independent and identically distributed

ISI: Intersymbol Interference

ITU: International Telecommunication Union

LTE: Long Term Evolution

MCS: Modulation and Coding Schemes

MIMO: Multiple Input Multiple Output

MU-MIMO: Multi-User MIMO

NAK: Negative Acknowledgment

OFDM: Orthogonal Frequency Division Multiplexing

OFDMA: Orthogonal Frequency Division Multiple Access

p : Pole

PDP: Power Delay Profile

pds: power spectral density

PMI: Precoding Matrix

RB: Resource Block

RI: Rank Indicator

RTT: Round-Trip Time

ReTx: Retransmission

R_{xy} : Correlation between x and y

sBW: OFDM sub-carrier spacing

SC-FDMA: Single-carrier FDMA

SINR: Signal to Interference plus Noise Ratio

SoS: Sum-of-Sinusoids

SU-MIMO: Single-User MIMO

T_c : Coherence time

t_{cp} : cyclic prefix time

TDD: Time-Division Duplex

T_s : Time duration of a transmission symbol

TTI: Transmission Time Interval

t_u : Useful symbol time

UE : User's Equipment

UHF: Ultra High Frequencies

UMTS: Universal Mobile Telephone System

UL: Up Link

V_m : Mobile speed

VoIP: Voice over IP

WiMAX: Worldwide Interoperability for Microwave Access

REFERENCES

- [1] 3G Americas. HSPA-LTE Advanced Sept 2009,
http://www.3gamericas.org/documents/3G_Americas_RysavyResearch_HSPA-LTE_Advanced_Sept2009.pdf
- [2] SAE-The core network for LTE, Ericsson:
http://www.3g4g.co.uk/Lte/SAE_Pres_0804_Ericsson.pdf
- [3] Cyril-Daniel Iskander, "A Matlab-based Object-Oriented Approach to Multipath Fading Channel Simulation", Hi-Tek Multisystems, 21 February 2008
- [4] Monghal, G.; Kovacs, I.Z.; Pokhariyal, A.; Pedersen, K.I.; Rosa, C.; Mogensen, P.E.; , "Fast Fading Implementation Optimization in an OFDMA System Simulator," *Vehicular Technology Conference, 2007. VTC2007-Spring. IEEE 65th* , vol., no., pp.1214-1218, 22-25 April 2007
- [5] Sorensen, T.B.; Mogensen, P.E.; Frederiksen, F.; , "Extension of the ITU channel models for wideband (OFDM) systems," *Vehicular Technology Conference, 2005. VTC-2005-Fall. 2005 IEEE 62nd* , vol.1, no., pp. 392- 396, 28-25 Sept., 2005
- [6] B. Sklar, "Rayleigh fading channels in mobile digital communications systems part I: characterization", *IEEE Commun. Mag.*, pp. 90-100, July 1997
- [7] Young, D.J.; Beaulieu, N.C.; , "The generation of correlated Rayleigh random variates by inverse discrete Fourier transform," *Communications, IEEE Transactions on* , vol.48, no.7, pp.1114-1127, Jul 2000
- [8] M. K. Simon and M.-S. Alouini, *Digital Communications Over Fading Channels*, Wiley
- [9] Matthias Patzold. 2003. *Mobile Fading Channels*. John Wiley & Sons, Inc., New York, NY, USA
- [10] L. C. Godara, *Handbook of Antennas in Wireless Communications*. Boca Raton, FL: CRC Press, 2002
- [11] Roth, S. Frame Allocation and Scheduling for Relay Networks in the LTE Advanced Standard, 2010 (creo que es una tesis o un pfc)
- [12] S. Parkvall, *3G Evolution –HSPA and LTE for Mobile Broadband*, Ericsson Research
- [13] H. Holma and A. Toskala, *LTE for UMTS — OFDMA and SC-FDMA Based Radio Access*, Wiley, 2009
- [14] C. S. Patel and G.L. Stuber, "Channel estimation for amplify and forward relay based cooperation diversity systems," *IEEE Trans. Wireless Commun.*, vol. 6, no. 6, June 2007 (thesis)

- [15] Komninakis, C.;"A fast and accurate Rayleigh fading simulator, "Global Telecommunications Conference, 2003. GLOBECOM '03. IEEE , vol.6, no., pp. 3306-3310 vol.6, 1-5 Dec. 2003
- [16] Encyclopaedia Britannica,<http://www.britannica.com/>
- [17] Cprogramming.com,
<http://www.cprogramming.com/tutorial/computersciencetheory/sortcomp.html>
- [18] William H. Press, Saul A. Teukolsky, William T. Vetterling, and Brian P. Flannery. 2007. *Numerical Recipes 3rd Edition: The Art of Scientific Computing* (3 ed.). Cambridge University Press, New York, NY, USA
- [19] W. C. Jakes, "Microwave Mobile Communications". Piscataway, NJ: IEEE Press, 1994
- [20] Ekstrom, H.; Furuskar, A.; Karlsson, J.; Meyer, M.; Parkvall, S.; Torsner, J.; Wahlqvist, M.; , "Technical solutions for the 3G long-term evolution," *Communications Magazine, IEEE* , vol.44, no.3, pp. 38- 45, March 2006
- [21] Tachikawa, K.; , "A perspective on the evolution of mobile communications," *Communications Magazine, IEEE* , vol.41, no.10, pp. 66- 73, Oct 2003
- [22] FRANSMAN M. (2003): "Knowledge and industry evolution: The mobile communications industry evolved largely by getting things wrong", paper presented at the DRUID summer conference, 2003.
- [23] 3GPP Technical Specification 36.211, 'Physical Channels and Modulation (Release 8)', www.3gpp.org.
- [24] D. Astely, E. Dahlman, A. Furuskar, Y. Jading, M. Lindstrom, S. Parkvall, "LTE: the evolution of mobile broadband," *Communications Magazine, IEEE* , vol.47, no.4, pp.44-51, April 2009
- [25] 3GPP Technical Specification 36.101, 'User Equipment (UE) Radio Transmission and Reception (Release 8)', www.3gpp.org
- [26] A. Ghosh, J. Zhang, J. G. Andrews, and R. Muhamed, *Fundamentals of LTE*. Prentice-Hall, 2010
- [27] T. Nakamura, " Proposal for Candidate Radio Interface Technologies for IMT-Advanced Based on LTE Release 10 and Beyond", 3GPP 2009,
http://www.3gpp.org/IMG/pdf/2009_10_3gpp_IMT.pdf
- [28] Source: 3GPP Multi-member analysis
- [29] G. Fritze, "SAE - The Core Network for LTE", Ericsson Austria GmbH,
http://www.3g4g.co.uk/Lte/SAE_Pres_0804_Ericsson.pdf
- [30] Document from IEEE Macau,

http://ieeemacau.eee.umac.mo/ieee_student/history%20of%20mobile%20phone.htm

[31] Long Term Evolution (LTE): Overview of LTE Air-Interface Technical White Paper. Motorola,

<http://business.motorola.com/experiencelte/pdf/LTEAirInterfaceWhitePaper.pdf>

[32] Kushner, H. J.; Whiting, P.A., "Convergence of proportional-fair sharing algorithms under general conditions", IEEE Transactions on Wireless Communications, 3 (4): 1250-1259, July 2004.



Escola d'Enginyeria de Telecomunicació i
Aeroespacial de Castelldefels

UNIVERSITAT POLITÈCNICA DE CATALUNYA

ANNEX A

TITLE: LTE Performance Evaluation with Realistic Channel Quality Indicator Feedback

MASTER DEGREE: Master in Science in Telecommunication Engineering & Management

AUTHOR: Mathew William Churchman Barata

DIRECTOR: Mario García Lozano

DATE: April 29th 2011

ANNEX A

A.1 Evolution of mobile communications

This section does an overview of the evolution of mobile communications, from the first analogue cellular one to the fourth generation which implements LTE. This overview is going to be centred in the European evolution due to the location of the research. Figure A.1 shows the cellular telephony generation from the point of view of North America and Europe.

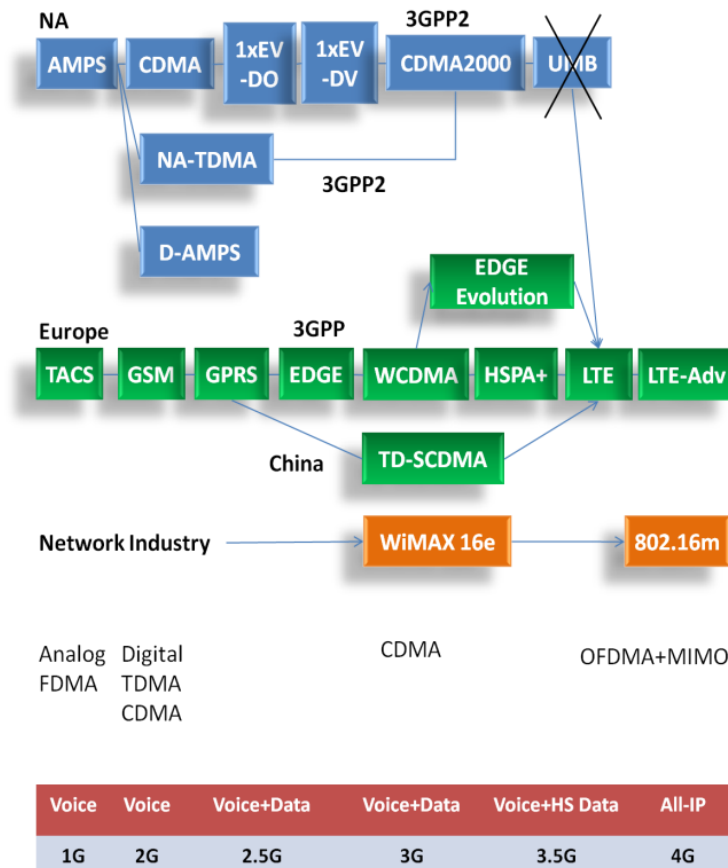


Figure A.1: Cellular telephony generations

A.1.1 First generation

The term 1G is the name given to the first generation of mobile telephone networks. These systems used analogue circuit-switched technology, with FDMA (Frequency Division Multiple Access), and worked mainly in the 800-900 MHz frequency bands. The networks had a low traffic capacity, unreliable handover, poor voice quality, and poor security [30].

These networks were the earliest cellular systems to be developed, and they relied on a network of distributed transceivers to communicate with the mobile phones. First generation phones were also analogue, used for voice calls only, and their signals were transmitted by the method of frequency modulation. These systems typically allocated one 25 MHz frequency band for the signals to be sent from the cell base station to the handset, and a second different 25 MHz band for signals being returned from the handset to the base station. These bands were then split into a number of communications channels, each of which would be used by a particular caller.

Until the early 1980s it was widely believed that mobile communications would not become a high-growth mass-consumption part of the telecommunications industry. Modern mobile communications are based on a cellular concept that allows the carrying capacity of the mobile network to be expanded by re-using frequencies in non-contiguous cells or by using better resource management technologies, thereby economising greatly on scarce spectrum. The first proposal to use cellular systems in the field of mobile communications was put forward in AT&T's Bell Laboratories in 1947 and discussed subsequently in a number of internal memoranda. The first publication on cellular communications emerged from Bell Labs in 1960. Only a decade later, in 1970, the first civilian standard for modern cellular telephony began to be specified in Scandinavia, leading to the Nordic Mobile Telephony (NMT) standard that was introduced in 1981 [22]. See figures A.2 a) and b).



Figure A.2: a) 1924. Bell Labs tested mobile radio telephony, b) Early 1970s-Bell System tested the cellular concept, which had already been used in a commercial system since 1969, c) 1956. Original mobile phone from SRA (Svenska Radioaktiebolaget), d) The Motorola Dyna-TAC from 1983 was the first handheld cellular phone

However, despite the advance of the technology and the possible uses it created, the general view in the 1970s and early 1980s was that mobile communications were unlikely to become high-growth segment. Depending on radio waves transmitted through the outside air between the handset and base station, mobile communications were believed to be based on an inferior transmission technology resulting in relatively high levels of interference and relatively low capacity and speed. In order to improve transmission performance, frontier research at the time focused on waveguides and later optical fibre that would guide light, rather than electro-magnetic radio signals, more efficiently thus providing levels of capacity and speed far in excess of what could be achieved using wireless communications. Furthermore, complementary technologies and assets also presented problems from the users' point of view. For example, the handsets were large, heavy and with limited battery-power.

A.1.2 Second generation

As analogue technologies began to be inefficient in contrast to digital systems, second generation mobile telephone networks (2G) were the logical next stage in the development of wireless systems after 1G, and they introduced for the first time a mobile phone system that used purely digital technology. The demands placed on the networks, particularly in the densely populated areas within cities, meant that increasingly sophisticated methods had to be employed to handle the large number of calls of users in movement, and so avoid the risks of interference and dropped calls at handoffs. Although many of the principles involved in a 1G system also apply to 2G - they both use the same cell structure - there are also differences in the way that the signals are handled, and the 1G networks are not capable of providing the more advanced features of the 2G systems, such as caller identity and text messaging.

In GSM 900, for example, two frequency bands of 25 MHz BW were initially used (extended later on). The band 890-915 MHz is dedicated to uplink communications from the mobile station to the base station, and the band 935-960 MHz is used for the DL communications from the base station to the mobile station. Each band is divided into 124 carrier frequencies, spaced 200 kHz apart, in a similar fashion to the FDMA method used in 1G systems. Then, each carrier frequency is further divided using TDMA into eight 577 μ s long time slots, every one of which represents one communication channel - the total number of possible channels available is therefore 124×8 , producing a theoretical maximum of 992 simultaneous conversations. In the USA, a different form of TDMA is used in the system known as IS-136 D-AMPS, and there is another US system called IS-95 (CDMAone), which is a spread spectrum code division multiple access (CDMA) system. CDMA is the technique used in 3G systems.

The evolution of the second generation is named 2.5G (Second Generation Enhanced), which is a generic term used to refer to a standard of wireless mobile telephone networks that lies somewhere between 2G and 3G.

The development of 2.5G has been viewed as a stepping-stone towards 3G, which was prompted by the demand for better data services and access to the Internet. In the evolution of mobile communications, each generation provides a higher data rate and additional capabilities, and 2.5G is no exception as it provides faster services than 2G, but not as fast or as advanced as the newer 3G systems.

Some observers have seen 2.5G as an alternative route to 3G, but this appears to be short-sighted as 2.5G is several times slower than the full 3G service. In technical terms 2.5G extends the capabilities of 2G systems by providing additional features, such as a packet-switched connection (GPRS) in the TDMA-based GSM system, and enhanced data rates (HSCSD and EDGE). But with lower speed rates, these enhancements permit data speeds of 64-144 kbps, which enables these phones to feature web browsing, the use of navigation and navigational maps, voice mail, fax, and the sending and receiving of large email messages.



Figure A.3: a) 1992. Nokia 1011. First commercially available GSM digital phone b) 1996. The Nokia 9000 Communicator. First mobile phone and handheld computer (PDA). from <http://www.nokia.com>, c) 2001. Ericsson R520m. First phone that supports fast General Packet Radio Service (GPRS) d) 2002. Nokia 6200. First EDGE phone

A.1.3 Third generation

Third generation (3G) mobile telephone networks are the next stage in the development of wireless communications technology. Significant features of 3G systems are that they support much higher data transmission rates and offer increased capacity, which makes them suitable for high-speed data applications as well as for the traditional voice calls. In fact, 3G systems are designed to process data, and since voice signals are converted to digital data, these results in speech being dealt with in much the same way as any other form of data. Third generation systems use packet-switching technology, which is more efficient and faster than the traditional circuit-switched systems, but they do require a somewhat different infrastructure to the 2G systems.

Compared to earlier mobile phones a 3G handset provides many new features, and the possibilities for new services are almost limitless, including many popular applications such as TV streaming, multimedia, videoconferencing, Web browsing, e-mail, paging, fax, and navigational maps.

Japan was the first country to introduce a 3G system, which was largely because the Japanese PDC networks were under severe pressure from the vast appetite in Japan for digital mobile phones. Unlike the GSM systems, which developed various ways to deal with demand for improved services, Japan had no 2.5G enhancement stage to bridge the gap between 2G and 3G, and so the move into the new standard was seen as a solution to their capacity problems.

It is generally accepted that CDMA is a superior transmission technology, when it is compared to the old techniques used in GSM/TDMA. WCDMA systems make more efficient use of the available spectrum, because the CDMA technique enables all base stations to use the same frequency. In the WCDMA system, the data is split into separate packets, which are then transmitted using packet switching technology, and the packets are reassembled in the correct sequence at the receiver end by using the code that is sent with each packet. WCDMA has a potential problem, caused by the fact that, as more users simultaneously communicate with a base station, then a phenomenon known as cell breathing can occur. This effect means that the users will compete for the finite power of the base station's transmitter, which can reduce the cell's range – W-CDMA and cdma2000 have been designed to alleviate this problem.

The operating frequencies of many 3G systems will typically use parts of the radio spectrum in the region of approximately 2GHz which were not available to operators of 2G systems, and so are away from the crowded frequency bands currently being used for 2G and 2.5G networks. UMTS systems are designed to provide a range of data rates, depending on the user's circumstances, providing up to 144 kbps for moving vehicles (macrocellular environments), up to 384 kbps for pedestrians (microcellular environments) and up to 2 Mbps for indoor or stationary users (picocellular environments). In contrast, the data rates supported by the basic 2G networks were only 9.6 kbps, such as in GSM, which was inadequate to provide any sophisticated digital services.

The following step which is not considered fourth generation is named 3.5G. In Europe the new standards associated to this term is HSPA.

HSPA refers to networks that support both HSDPA and HSUPA. All new deployments today are HSPA, and many operators have upgraded their HSDPA networks to HSPA [1]. HSDPA, specified in 3GPP Release 5, is a high-performance, packet-data service that delivers peak theoretical rates of 14 Mbps. Peak user-achievable throughput rates in initial deployments are well over 1 Mbps and as high as 4 Mbps in some networks. The same radio carrier can simultaneously service UMTS voice and data users, as well as HSDPA data users. HSDPA achieves its high speeds through techniques similar to those that push EDGE performance past GPRS including higher order modulation, variable coding, and soft combining, as well as through the addition of powerful new techniques such as fast scheduling.

Whereas HSDPA optimizes DL performance, HSUPA—which uses the Enhanced Dedicated Channel (E-DCH)—constitutes a set of improvements that optimizes uplink . HSUPA is standardized in Release 6. It results in an approximately 85 percent increase in overall cell throughput on the uplink and more than 50 percent gain in user

throughput. HSUPA also reduces packet delays, a significant benefit resulting in much improved application performance on HSPA networks performance.

A.1.4 Fourth generation

The term 4G applies to networks that comply with the requirements of IMT-Advanced that are articulated in Report ITU-R M.2134. Some of the key requirements or statements include:

- Support for scalable BW up to and including 40 MHz
- Encouragement to support wider BWs (e.g., 100 MHz)
- Minimum DL peak spectral efficiency of 15 bps/Hz (assumes 4X4 MIMO)
- Minimum uplink peak spectral efficiency of 6.75 bps/Hz (assumes 2X4 MIMO)

A.1.4.1 Basic System Architecture Configuration

The core network architecture of LTE is System Architecture Evolution (SAE) differs from the previous systems in:

- Simplified architecture
- All IP Network (AIPN)
- Support for higher throughput and lower latency radio access networks (RANs)
- Support for, and mobility between, multiple heterogeneous RANs, including legacy systems as GPRS, but also non-3GPP systems (for example WiMAX)

The architecture can be divided into four main high level domains: Services domain, Evolved Packet Core Network (EPC), Evolved UTRAN (E-UTRAN) and the User Equipment (UE). The high level architectural domains are functionally equivalent to those in the existing 3GPP systems. The new architectural development is limited to Radio Access and Core Networks, the E-UTRAN and the EPC respectively. UE and Services domains remain architecturally intact, but functional evolution has also continued in those areas [13]. The EPC, E-UTRAN and UE represent the Internet Protocol (IP) Connectivity Layer [2]. This part of the system is also called the Evolved Packet System (EPS). The main function of this layer is to provide IP based connectivity, and it is highly optimized for that purpose only. See figure A.4.

The EPC will serve as equivalent of GPRS networks (via the Mobility Management Entity (MME), Serving Gateway and PDN Gateway subcomponents which form the SAE GW). The EPC/SAE framework is an evolution or migration of the 3GPP system to a higher-data-rate, lower-latency, packet-optimized system that supports multiple radio-access technologies [1].

The MME hosts the distribution of paging messages to the eNodeBs, the security control, the Idle state mobility control, the SAE bearer control and the Ciphering and integrity protection of NAS signalling. While the SAE Gateway hosts the Termination of U-plane packets and the switching of U-plane for support of UE mobility.

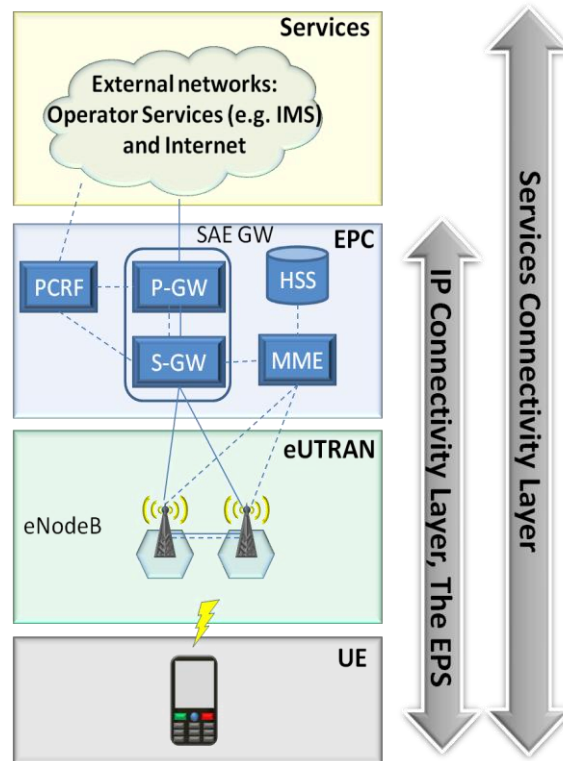


Figure A.4: System architecture for E-UTRAN only network

The only node in the E-UTRAN is the E-UTRAN Node B (eNodeB). The eNodeB is a radio base station which is in control of all radio related functions in the fixed part of the system. Base stations such as eNodeB are typically distributed throughout the networks coverage area, each eNodeB residing near the actual radio antennas. Functionally eNodeB acts as a layer 2 bridge between UE and the EPC, by being the termination point of all the radio protocols towards the UE, and relaying data between the radio connection and the corresponding IP based connectivity towards the EPC [29]. In this role, the eNodeB performs ciphering/deciphering of the UP data, and also IP header compression/decompression, which means avoiding repeatedly sending the same or sequential data in IP header. The eNodeB is also responsible for many Control Plane (CP) functions. The eNodeB is responsible for the Radio Resource Management (RRM), i.e. controlling the usage of the radio interface, which includes, for example, allocating resources based on requests, prioritizing and scheduling traffic according to required Quality of Service (QoS), and constant monitoring of the resource usage situation.

As a summary, the eNodeB hosts the following functions [2]:

- Radio Resource Management
 - Radio Bearer Control
 - Radio Admission Control
 - Connection Mobility Control
 - UEs in both uplink and DL Dynamic allocation of resources to (scheduling)
- IP header compression and encryption of user data stream
- Selection of an MME at UE attachment
- Routing of User Plane data towards SAE Gateway
- Measurement and measurement reporting configuration for mobility and scheduling

A.2 Simulation results

This section presents the simulation results which have not been showed in the main master thesis document: The ideal static LTE system simulator results and the assigned transport format (CQI) of the main simulations.

A.2.1 Ideal static LTE system simulator results

As mentioned in the main document, the dynamic LTE system simulator has been developed starting upon a static one. This static system simulator does not incorporate the realistic features introduced in this project so it works over theoretical assumptions. Due to this reason the obtained results are better. It is also necessary to take into account that the dynamic simulator only evaluates the users of one cell, while the static simulator evaluates all the cells with an average of 25 users per cell. For this reason more results have been obtained leading to a better definition in the CDF of the users' throughput and the assigned CQI index (figure A.5).

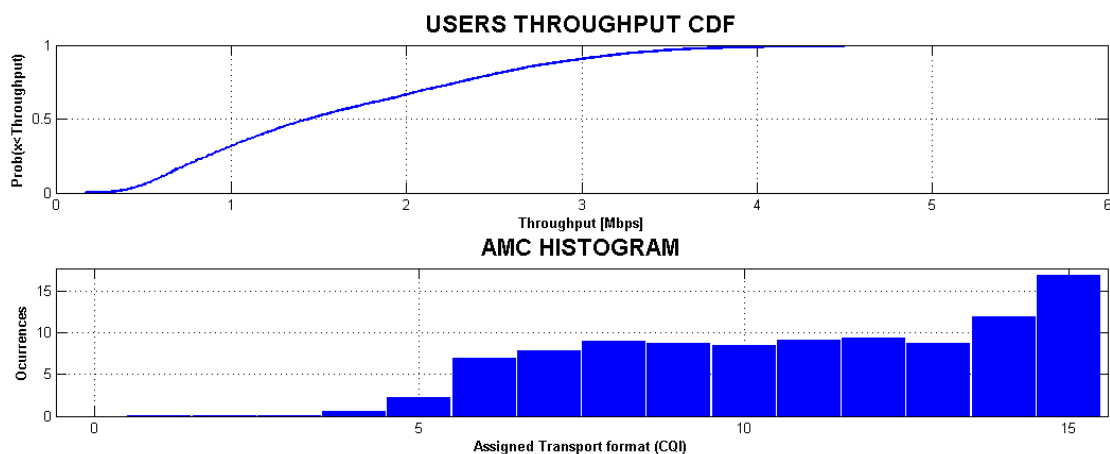


Figure A.5: Ideal static LTE system simulator results. Users' throughput CDF and percentage of assigned transport format (CQI).

A.2.2 Assigned transport format (CQI)

This section presents the percentage of assigned CQI index and the resulting value of the assigned CQI index which has led to a correct reception of the transport block. The figures show the results for 3 and 120 Km/h for each CQI reporting method.

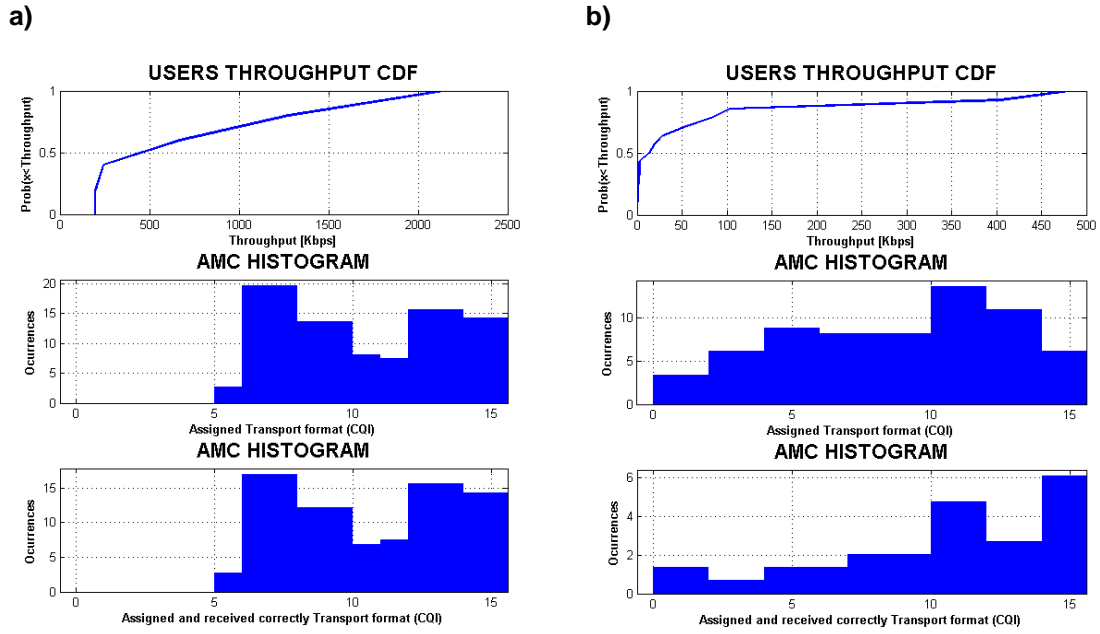


Figure A.6: Ideal feedback. **a)** 3Km/h, **b)** 120Km/h

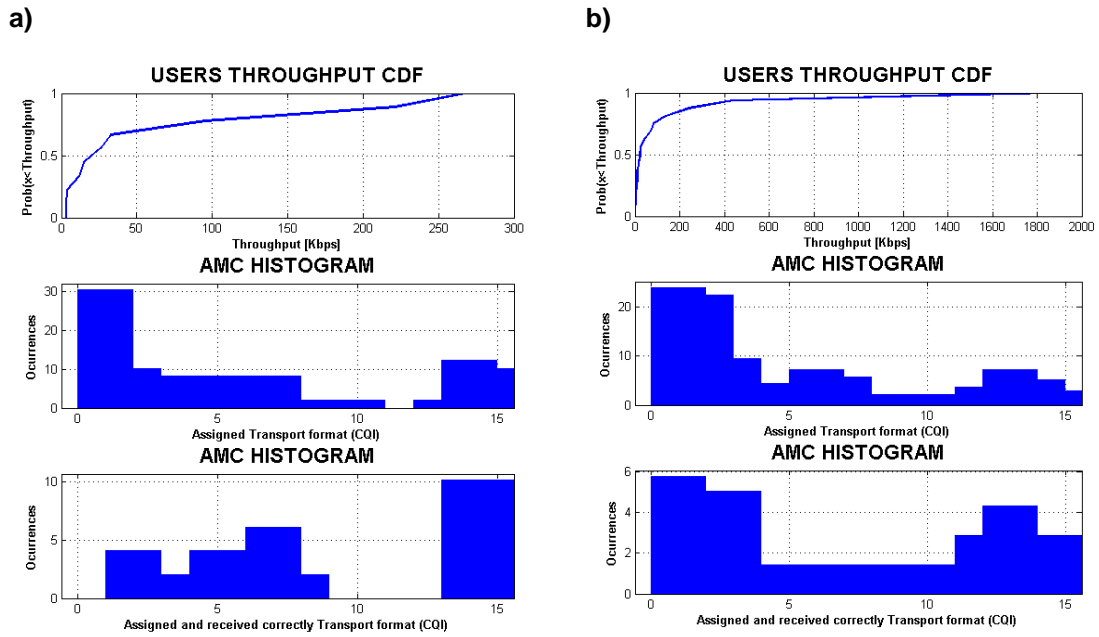


Figure A.7: Wideband feedback. **a)** 3Km/h, **b)** 120Km/h

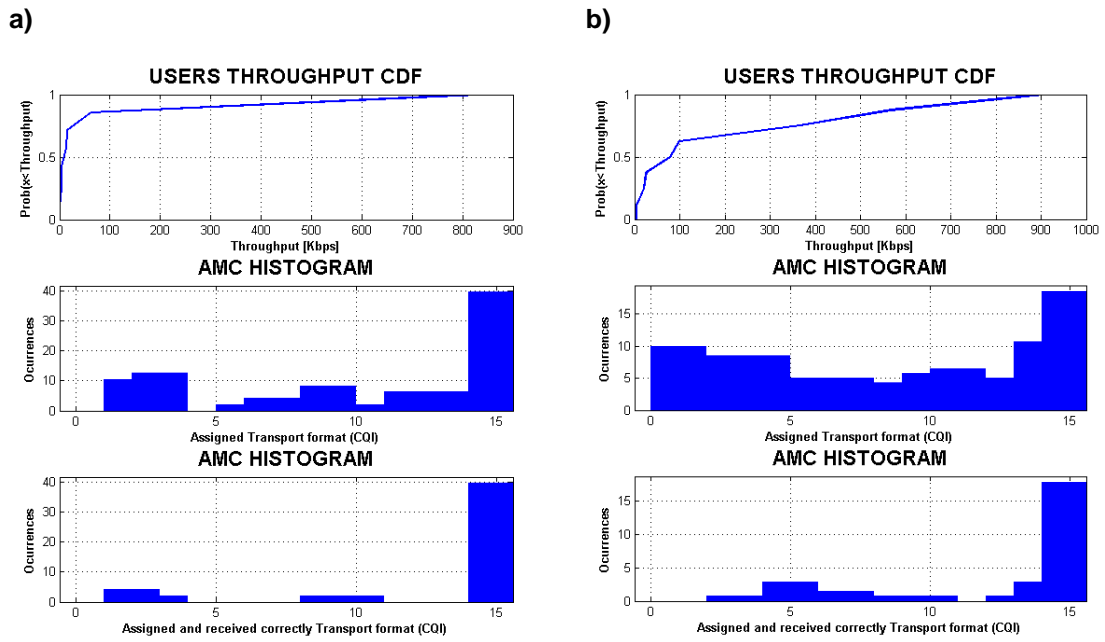


Figure A.8: Best-M feedback. k=6, M=4. a) 3Km/h, b) 120Km/h

A.3 Simulation parameters

The simulation parameters per tab are shown in the following screenshots.

A.3.1 Layout and users

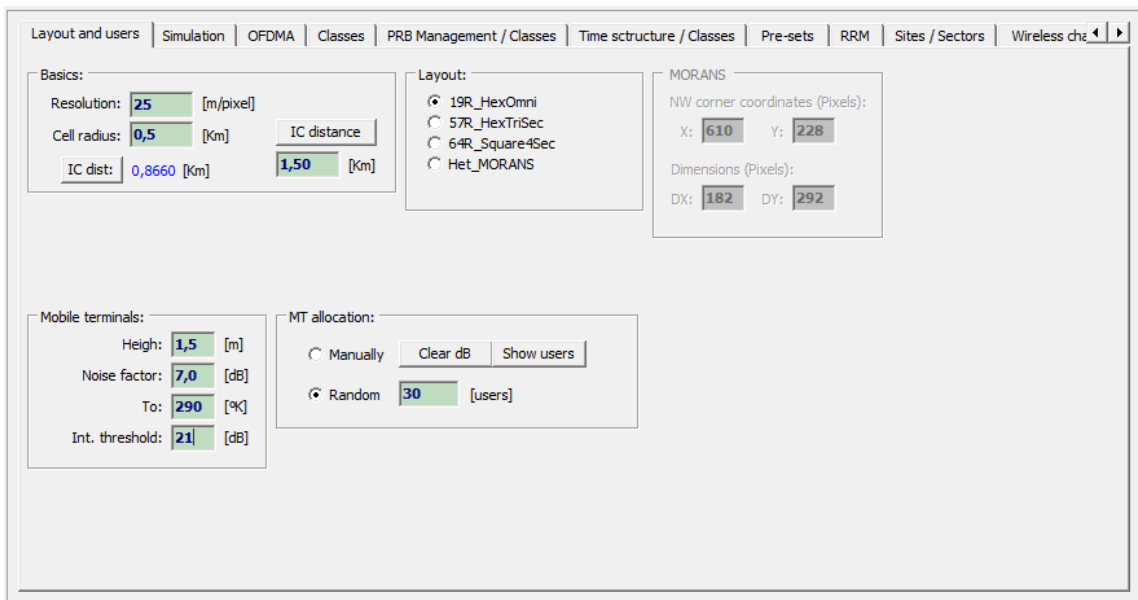


Figure A.9: Simulation parameters. Layout and users

A.3.2 Simulation

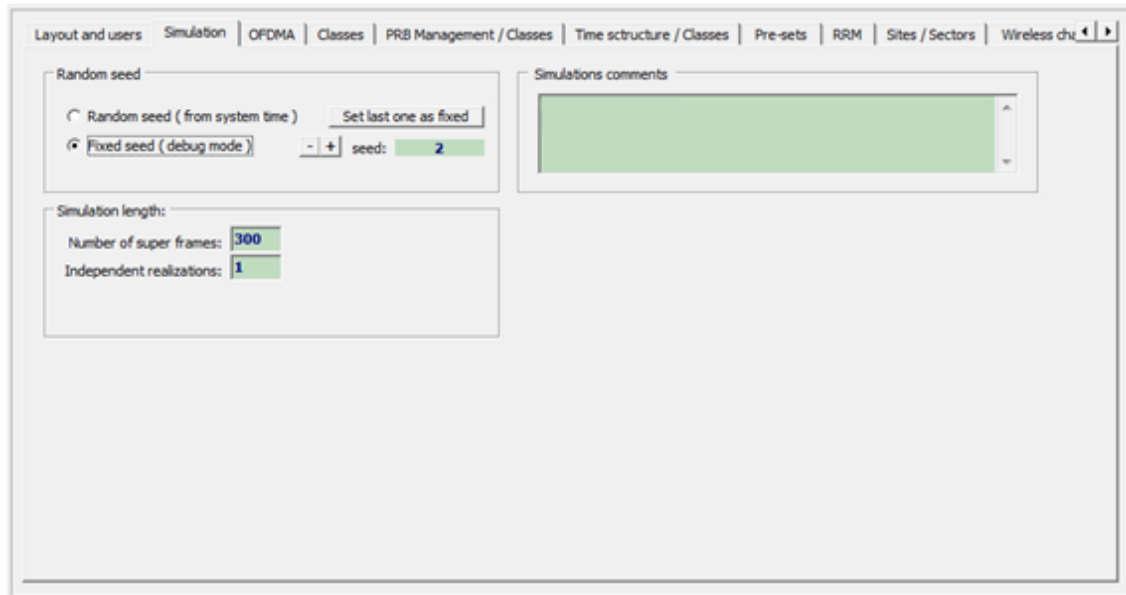


Figure A.10: Simulation parameters. Simulation

A.3.3 OFDMA



Figure A.11: Simulation parameters. OFDMA

A.3.4 Classes

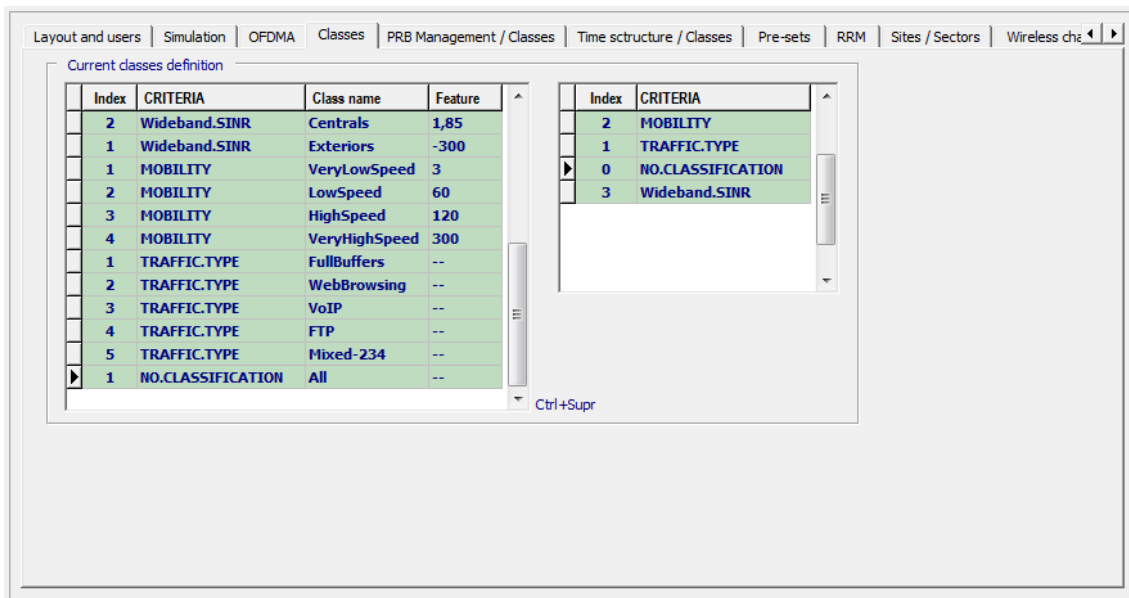


Figure A. 12: Simulation parameters. Classes

A.3.5 RRM

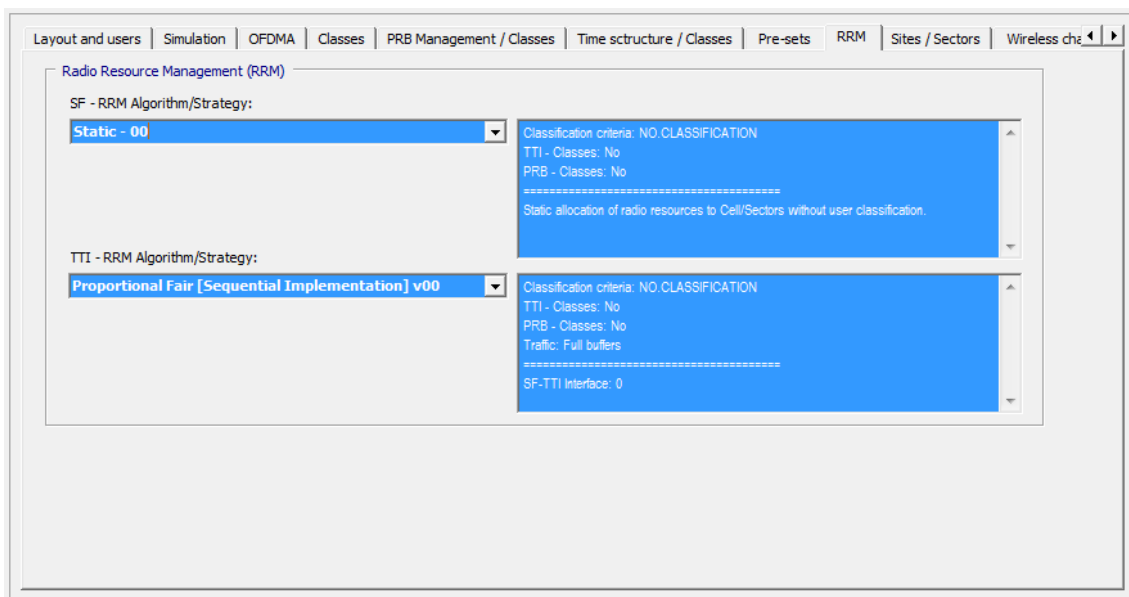


Figure A. 13: Simulation parameters. Classes

A.3.6 Sites/Sectors

Layout and users | Simulation | OFDMA | Classes | PRB Management / Classes | Time structure / Classes | Pre-sets | RRM | Sites / Sectors | Wireless channel

Sites

ID	X	Y	h [m]
0	85	90	15
1	85	56	15
2	55	73	15
3	55	107	15
4	85	124	15
5	115	107	15

Default height: 15.0 [m]
Show position Site: N/A

Cells/Sectors

ID	Site ID	Power [dBm]	Ant. model	Ant. direction [°]	Downtilt
0	0	43	Kathrein_800_10147_VPol Omni	0	0
1	1	43	Kathrein_800_10147_VPol Omni	0	0
2	2	43	Kathrein_800_10147_VPol Omni	0	0
3	3	43	Kathrein_800_10147_VPol Omni	0	0
4	4	43	Kathrein_800_10147_VPol Omni	0	0
5	5	43	Kathrein_800_10147_VPol Omni	0	0

Default total power per Cell/Sector: 43 [dBm]
Default antenna downtilt: 0 [°]
Default antenna model: Kathrein_800_10147_VPol Omni

Figure A. 14: Simulation parameters. Sites/Sectors

A.3.7 Wireless Channel

Simulation | OFDMA | Classes | PRB Management / Classes | Time structure / Classes | Pre-sets | RRM | Sites / Sectors | Wireless channel | PHY

SMALL SCALE - Frequency selective fading

Pre-loaded channel models for multi-path fading:
[Frequency selectiveness]
ITU - Extended pedestrian B (EPB) [32,55 ns]

LARGE SCALE - Path Loss

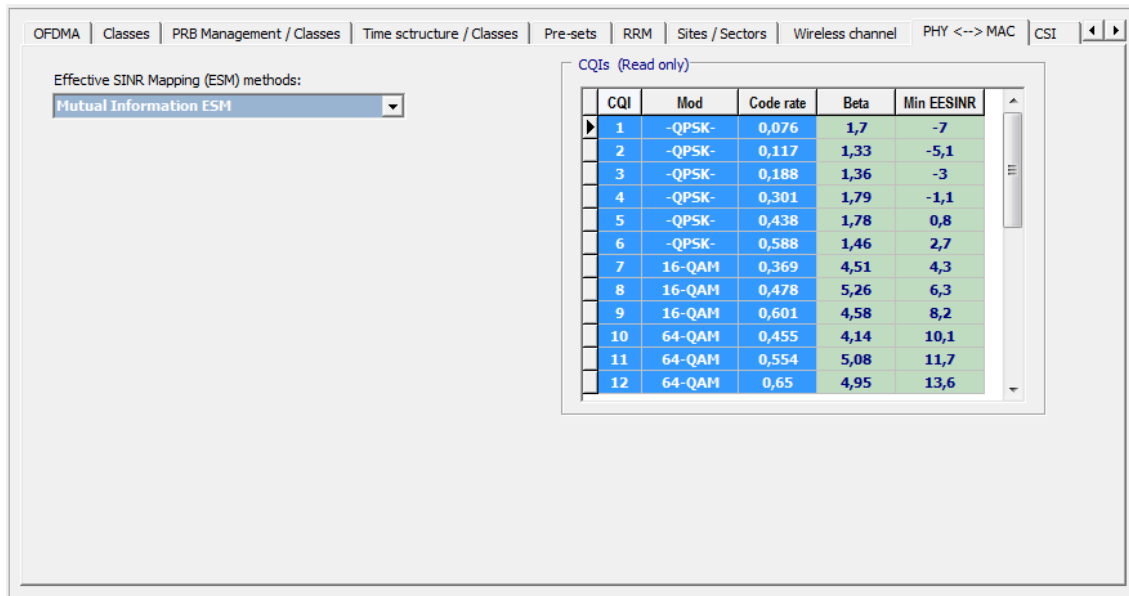
Carrier frequency: 2140,00 [MHz]
Macro-Cellular models:
Urban Macrocellular - 3GPP

LARGE SCALE - Shadowing:

Apply shadow fading to users

Figure A. 15: Simulation parameters. Wireless Channel

A.3.8 PHY-MAC



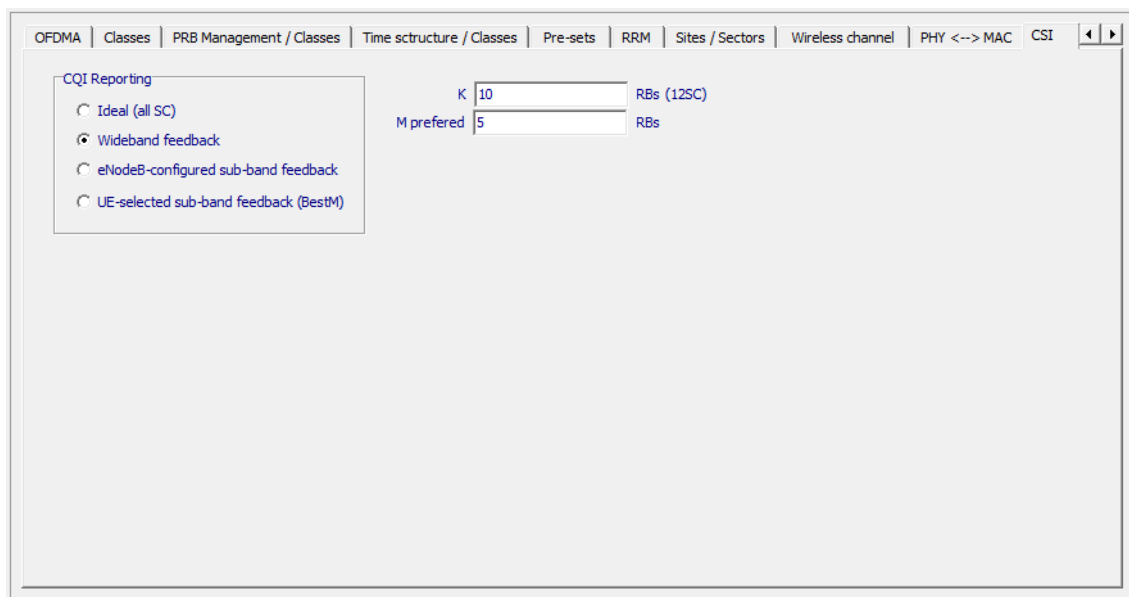
Effective SINR Mapping (ESM) methods:
Mutual Information ESM

CQIs (Read only)

CQI	Mod	Code rate	Beta	Min EESINR
1	-QPSK-	0,076	1,7	-7
2	-QPSK-	0,117	1,33	-5,1
3	-QPSK-	0,188	1,36	-3
4	-QPSK-	0,301	1,79	-1,1
5	-QPSK-	0,438	1,78	0,8
6	-QPSK-	0,588	1,46	2,7
7	16-QAM	0,369	4,51	4,3
8	16-QAM	0,478	5,26	6,3
9	16-QAM	0,601	4,58	8,2
10	64-QAM	0,455	4,14	10,1
11	64-QAM	0,554	5,08	11,7
12	64-QAM	0,65	4,95	13,6

Figure A. 16: Simulation parameters. PHY-MAC

A.3.9 CSI



CQI Reporting

Ideal (all SC)
 Wideband feedback
 eNodeB-configured sub-band feedback
 UE-selected sub-band feedback (BestM)

K RBs (12SC)
M preferred RBs

Figure A.17: Simulation parameters. PHY-MAC

A.4 LTE frequency bands

LTE Band	Uplink eNode B receive UE transmit	DL eNode B transmit UE receive	Duplex mode
1	1920 MHz – 1980 MHz	2110 MHz – 2170 MHz	FDD
2	1850 MHz – 1910 MHz	1930 MHz – 1990 MHz	FDD
3	1710 MHz – 1785 MHz	1805 MHz – 1880 MHz	FDD
4	1710 MHz – 1755 MHz	2110 MHz – 2155 MHz	FDD
5	824 MHz – 849 MHz	869 MHz – 894 MHz	FDD
6	830 MHz – 840 MHz	875 MHz – 885 MHz	FDD
7	2500 MHz – 2570 MHz	2620 MHz – 2690 MHz	FDD
8	880 MHz – 915 MHz	925 MHz – 960 MHz	FDD
9	1749.9 MHz – 1784.9 MHz	1844.9 MHz – 1879.9 MHz	FDD
10	1710 MHz – 1770 MHz	2110 MHz – 2170 MHz	FDD
11	1427.9 MHz – 1452.9 MHz	1475.9 MHz – 1500.9 MHz	FDD
12	698 MHz – 716 MHz	728 MHz – 746 MHz	FDD
13	777 MHz – 787 MHz	746 MHz – 756 MHz	FDD
14	788 MHz – 798 MHz	758 MHz – 768 MHz	FDD
17	704 MHz – 716 MHz	734 MHz – 746 MHz	FDD
18	815 MHz – 830 MHz	860 MHz – 875 MHz	FDD
19	830 MHz – 845 MHz	875 MHz – 890 MHz	FDD
...			
33	1900 MHz – 1920 MHz	1900 MHz – 1920 MHz	TDD
34	2010 MHz – 2025 MHz	2010 MHz – 2025 MHz	TDD
35	1850 MHz – 1910 MHz	1850 MHz – 1910 MHz	TDD
36	1930 MHz – 1990 MHz	1930 MHz – 1990 MHz	TDD
37	1910 MHz – 1930 MHz	1910 MHz – 1930 MHz	TDD
38	2570 MHz – 2620 MHz	2570 MHz – 2620 MHz	TDD
39	1880 MHz – 1920 MHz	1880 MHz – 1920 MHz	TDD
40	2300 MHz – 2400 MHz	2300 MHz – 2400 MHz	TDD

Table A.1: LTE frequency bands